
Keep Searching, the Optimum Is Out There!

Anonymous Author(s)

Affiliation
Address
email

Abstract

1 Achieving robust *anytime performance* in combinatorial optimization requires a
2 delicate balance between exploration and exploitation. Effective strategies in the
3 optimization literature typically involve: (i) evolving multiple search trajectories
4 for each instance, (ii) preserving diversity among them, and (iii) exploring the
5 entire search space in a structured manner. Most Neural Combinatorial Optimiza-
6 tion (NCO) methods, however, rely on either simple constructive heuristics or
7 single-trajectory local search, causing them to underperform when compared to
8 state-of-the-art methods. In this work, we introduce a collaborative multi-agent
9 system that effectively balances exploration and exploitation, bridging the gap be-
10 tween learning-based and classical methods, and achieving unprecedented anytime
11 performance in NCO. Each agent iteratively refines a candidate solution while
12 sharing information through a centralized memory, promoting both cooperation
13 and search diversity. When an agent becomes trapped in a local optimum, it dis-
14 cards its current solution and uses a conditioned constructive network to generate
15 a new, high-quality solution that differs from those of other agents. Empirical
16 evaluations on multiple binary combinatorial benchmarks, including Maximum
17 Cut and Maximum Independent Set, show that our framework achieves superior
18 anytime performance compared to existing NCO methods and improves upon the
19 state-of-the-art specialized solvers.

20

1 Introduction

21 Neural Combinatorial Optimization (NCO) [Bengio et al., 2021, Mazyavkina et al., 2021, Bello
22 et al., 2016] represents an emerging framework that aims to address Combinatorial Optimization
23 Problems (COPs) through Neural Networks (NN) in an end-to-end manner. The core premise of
24 NCO is its ability to perform a *train-once, infer-multiple-times* approach, where a trained NN model
25 can generalize to unseen problem instances without necessitating retraining for each new instance.
26 Making NCO approaches suitable for scenarios where rapid inference over many instances is required,
27 such as online decision-making systems [Luo et al., 2024], real-time applications [Cappart et al.,
28 2023], or large-scale optimization pipelines [Zhou et al., 2024].

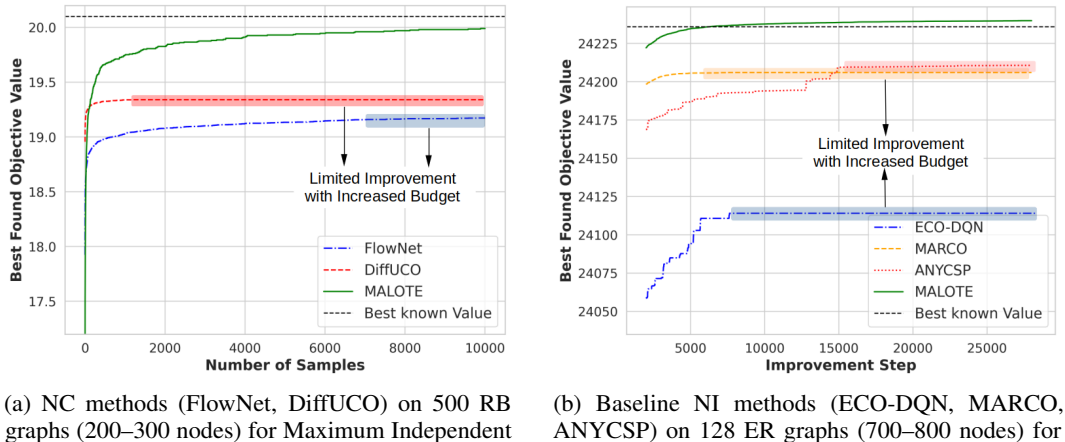
29 Early NCO approaches focused primarily on constructing solutions from scratch using neural net-
30 works to build approximate solutions in an autoregressive fashion. These methods, known as *Neural*
31 *Constructive* (NC) methods [Vinyals et al., 2015, Bello et al., 2016, Kool et al., 2018, Kwon et al.,
32 2020], initiate the process with an empty structure and incrementally add one component at a time
33 until a complete and feasible solution is formed. Although effective, NC methods are inherently
34 limited by the construction of a single solution: they commit early to substructures without the
35 ability to revise decisions [Sun et al., 2024]. This myopic search behavior limits exploration, reduces
36 solution diversity, and hampers scalability to larger or more complex instances [Son et al., 2025].

37 To mitigate the exploration limitations of NC methods, the research community has developed *Neural*
38 *Improvement* (NI) methods [Chen and Tian, 2019, Lu et al., 2019, Barrett et al., 2020, Wu et al., 2021].

39 Inspired by classical local search heuristics [Blum and Roli, 2003], NI methods use NNs to iteratively
 40 refine a single candidate solution by modifying specific components. Although this enables exploring
 41 the local neighborhood, the search often remains confined to a narrow region: once a promising area
 42 is identified, the method tends to exploit it excessively, limiting broader exploration [Garmendia et al.,
 43 2023].

44 These issues in NCO and the success of classical optimization techniques highlights a critical gap.
 45 The most successful combinatorial optimization algorithms, such as metaheuristics [Blum and Roli,
 46 2003] and exact solvers [Gurobi Optimization, LLC, 2023], often rely on three key principles: (i)
 47 maintaining a diverse population of candidate solutions [Mitchell, 1998, Bonyadi and Michalewicz,
 48 2017], (ii) promoting diversity among individual search agents [Baste et al., 2022, Ren et al., 2024],
 49 and (iii) systematically exploring the search space in a structured way [Modaresi et al., 2020, Jooken
 50 et al., 2023]. Together, these strategies enhance the robustness of the search process and help prevent
 51 premature convergence to suboptimal regions.

52 Yet, most existing NCO methods do not incorporate these principles, leading to limited *anytime*
 53 performance, i.e., the ability to improve solutions over time. As shown in Figure 1, previous NCO
 54 approaches struggle to further improve these solutions when given additional computational budgets.



(a) NC methods (FlowNet, DiffUCO) on 500 RB graphs (200–300 nodes) for Maximum Independent Set.

(b) Baseline NI methods (ECO-DQN, MARCO, ANYCSP) on 128 ER graphs (700–800 nodes) for Maximum Cut.

Figure 1: Average objective values of the best solutions found by (a) NC and (b) NI methods. Plateaus indicate periods of stagnation despite continued computation. Results include our method (detailed later) to illustrate the performance gap motivating this work.

55 Our goal is to advance the anytime performance of NCO models by introducing more sophisticated
 56 techniques capable of outperforming current state-of-the-art designs. To this end, we propose *Multi-*
 57 *Agent Learning for Optimization with Trajectory Exploration* (MALOTE), a collaborative multi-agent
 58 reinforcement learning framework. MALOTE deploys multiple search agents in parallel, each
 59 improving a candidate solution while sharing information through a centralized memory that prevents
 60 revisiting previously explored solutions. To enhance exploration of the search space, each agent is
 61 equipped with an exploration module that activates when progress stalls in a non-improving region.
 62 Upon activation, the exploration module discards the agent’s current solution and generates a new,
 63 high-quality candidate that is explicitly diverse from those of other agents, using a conditioned neural
 64 constructive network.

65 MALOTE is designed to be broadly applicable across different combinatorial optimization prob-
 66 lems. In this work, we validate its effectiveness on two representative problems, Maximum Cut
 67 (MC) [Dunning et al., 2018] and Maximum Independent Set (MIS) [Lawler et al., 1980]. We also
 68 provide practical guidelines for extending MALOTE to alternative problems. Experimental results
 69 show that MALOTE not only surpasses previous state-of-the-art problem-specific algorithms on
 70 several benchmarks, but also exhibits strong generalization, achieving these results despite being
 71 trained on smaller graphs.

72 The main contributions of this paper are as follows. (a) We introduce *Multi-Agent Learning for*
 73 *Optimization with Trajectory Exploration* (MALOTE), a novel multi-agent framework augmented

74 with a shared memory component. (b) We design a dual-module agent architecture comprising
75 a first module for iterative improvement of candidate solutions, and a second module to enable
76 global exploration by restarting the search when agents get stuck in non-improving regions. (c) We
77 introduce a novel conditioned Neural Constructive (cNC) network, that generates new solutions
78 conditioned by an exploration weight, which dynamically adjusts the emphasis between optimizing
79 solution quality and exploring diverse solution spaces. (d) We demonstrate that a single trained
80 model can generalize across graph sizes and distributions, highlighting strong transfer capabilities.
81 (e) We validate MALOTE on two classic combinatorial optimization problems: Maximum Cut and
82 Maximum Independent Set. (f) We conduct comprehensive evaluations by benchmarking MALOTE
83 against exact methods, heuristics, metaheuristics, learning-based approaches, and ablation studies to
84 assess the impact of each component.

85 2 Related Work

86 In this section, we review the main contributions in NCO, structured around two core methodological
87 families: Neural Constructive (NC) and Neural Improvement (NI) approaches. We mention the
88 key limitations of these methods and examine how recent developments have addressed them with
89 memory-based strategies and multi-agent architectures.

90 **Neural Constructive methods.** Initial NC proposals by Vinyals et al. [2015] and Bello et al.
91 [2016] introduced the Pointer Network, which constructs approximate solutions for the Traveling
92 Salesperson Problem using Supervised Learning (SL) and Reinforcement Learning (RL), respectively.
93 Subsequently, Khalil et al. [2017] proposed the structure2vec (S2V) architecture, capable of repre-
94 senting the graph structure of various COPs and training it with Q-learning. These were followed
95 by a large number of incremental works, which extended the NC pipeline to different problems,
96 such as the Maximum Cut [Barrett et al., 2022], the Maximum Independent Set [Ahn et al., 2020]
97 and Job Shop Scheduling Problem [Zhang et al., 2020]; or using improved neural architectures,
98 such as Graph Neural Networks [Cappart et al., 2023] or Transformers [Bresson and Laurent, 2021].
99 Moreover, apart from SL and RL paradigms, the NCO field has recently seen a growing interest
100 in generative sampling frameworks based on Unsupervised Learning (UL), particularly through
101 diffusion probabilistic models [Sun et al., 2023, Sun and Yang, 2023, Sanokowski et al., 2024].

102 Despite these advances, previously proposed NC methods remain limited due to their inherently
103 Markovian structure, which ignores information from previously generated solutions. As a result,
104 they are prone to redundancy, often producing similar or even duplicate outputs.

105 **Neural Improvement Methods.** Common architectures used in NI include Long Short-Term
106 Memory (LSTM) networks [Chen and Tian, 2019], GNNs [Barrett et al., 2020] and attention-based
107 models [Lu et al., 2019, Hottung and Tierney, 2020].

108 For instance, Chen and Tian [2019] use an LSTM to score regions for modification and select the
109 corresponding rules. Lu et al. [2019] apply attention mechanisms to choose local operators for the
110 capacitated vehicle routing problem. Similarly, Hottung and Tierney [2020] propose a large neural
111 neighborhood search that uses attention to destroy and repair solution segments. Wu et al. [2021]
112 train policies to select node pairs for applying local operators like 2-opt for routing problems, while
113 da Costa et al. [2020] extend this approach to k-opt operators.

114 As the mentioned NC works, these NI approaches lack mechanisms to account for previously
115 visited solutions, making them susceptible to repetitive cycles and revisiting identical or similar solu-
116 tions [Garmendia et al., 2024]. This shortcoming makes it difficult for NI approaches to outperform
117 classical metaheuristics [Blum and Roli, 2003], which typically use mechanisms such as tabu lists or
118 population diversity to prevent revisiting the same solutions. To address this issue, recent work in
119 NCO has introduced explicit memory components to track and avoid previously explored solutions.

120 **Memory-based Neural Methods.** ECO-DQN [Barrett et al., 2022], an improvement-based frame-
121 work, tracks recent action histories to prevent immediate backtracking on solution modifications.
122 Similarly, MEMENTO [Chalumeau et al., 2024] extends NC methods by maintaining a repository of
123 past solutions and consulting this memory to avoid redundant exploration. Although these schemes
124 effectively reduce cyclic behavior along a single search trajectory, their reliance on one trajectory
125 often restricts exploration to narrow regions of the solution space. More expansive and diverse

126 exploration can be achieved by deploying multiple concurrent search trajectories, as realized in
127 multi-agent paradigms. Building upon these, MARCO Garmendia et al. [2024] introduces a memory
128 module that stores entire solutions along with their corresponding actions, while punishing the model
129 whenever it proposes a repetitive move during training.

130 **Multi-Agent Systems.** Some multi-agent methods fall under this broader taxonomy, although they
131 typically consist of agent populations where each agent is specialized for different types of problem
132 instances, rather than collaboratively tackling the same instance. For example, Poppy [Grinsztajn et al.,
133 2023] trains a population of RL agents, each tailored to a specific class of instances. PolyNet [Hottung
134 et al., 2024] generalizes this concept by using a single model conditioned on an input vector to select
135 among multiple policies.

136 Closer to collaborative approaches are methods that integrate neural networks into classical population-
137 based metaheuristics. DeepACO [Ye et al., 2024], for instance, combines neural networks with Ant
138 Colony Optimization (ACO) [Dorigo and Stützle, 2019], using learned heuristics to guide the search
139 and refine solutions. While ACO is inherently population-based, DeepACO primarily functions as
140 a neural enhancement layered on top of a conventional algorithm, rather than a fully end-to-end
141 population-based neural optimization method.

142 MARCO [Garmendia et al., 2024] can also be interpreted as a multi-agent system, where a parallel
143 population of NI agents tackles the same instance. However, these agents are not trained collabora-
144 tively: each maintains its own memory without access to shared information. As a result, exploration
145 remains localized, lacking global coordination or broader search strategies.

146 **3 Problem Formulation**

147 We consider a combinatorial optimization problem defined on an instance \mathcal{I} , consisting of a set of
148 elements V to be optimized under certain constraints and objectives. Let \mathcal{S} denote the set of all
149 feasible solutions for instance \mathcal{I} . Each solution $\mathbf{s} \in \mathcal{S}$ has an associated objective value $f(\mathbf{s})$, which
150 measures its quality. The goal is to find the *optimal solution*:

$$\mathbf{s}^* = \arg \max_{\mathbf{s} \in \mathcal{S}} f(\mathbf{s}),$$

151 where the maximization (or minimization, depending on the problem) is performed over all feasible
152 solutions in \mathcal{S} .

153 **4 MALOTE**

154 In this section, we introduce **MALOTE** (*Multi-Agent Learning for Optimization with Trajectory*
155 *Exploration*), a multi-agent reinforcement learning framework [Busoniu et al., 2008, Albrecht et al.,
156 2024] designed for NCO. A general overview of the framework is shown in Figure 2.

157 Formally, we define a population of RL agents $\mathcal{A} = \{A_1, A_2, \dots, A_k\}$, where each agent A_i
158 maintains a candidate solution $\mathbf{s}_i \in \mathcal{S}$.

159 In each iteration t , an agent A_i proposes an action that modifies its current solution \mathbf{s}_i^t to produce
160 a (potentially better) new solution \mathbf{s}_i^{t+1} . Depending on the specific combinatorial problem, these
161 actions may include operations such as adding, removing, swapping, or flipping the elements or their
162 values within the solution, or even replacing entirely the candidate solution with a new one. These
163 new solutions are stored in a shared memory \mathcal{M} accessible by the entire population (see the left
164 section of Figure 2).

165 To determine the action, each agent receives a representation of the current optimization process,
166 referred to as the state \mathbf{x}^t . The state \mathbf{x}_i^t of agent A_i comprises:

- 167 • **\mathcal{I} : Problem Instance.** Includes the complete problem description, such as the graph
168 structure (adjacency matrix) and node- or edge-features, which define all constraints and
169 parameters.
- 170 • **\mathbf{s}_i^t : Current Candidate Solution.** Represents the current attempt of agent A_i in the solution
171 space.

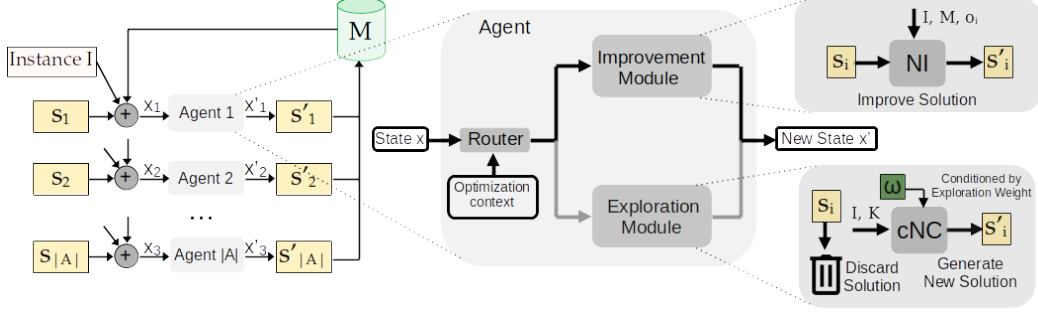


Figure 2: Pipeline of MALOTE. Each agent i receives a state \mathbf{x}_i^t , comprising the problem instance \mathcal{I} , current solution \mathbf{s}_i^t , memory-based historical data \mathcal{M} and the optimization context \mathbf{o}_i^t . A router selects the appropriate module: the *improvement* module refines \mathbf{s}_i^t using a neural improvement model, while the *exploration* module replaces it with a new solution generated by a conditioned neural constructive model. This model balances quality and diversity with respect to a memory subset \mathcal{K} , guided by an exploration weight ω . The resulting solution \mathbf{s}_i^{t+1} is stored in memory and integrated into the updated state \mathbf{x}_i^{t+1} .

- **\mathcal{M} : Shared Memory.** A centralized repository for storing all solutions explored by the agents, enabling shared learning and avoidance of duplicate work.
- **\mathbf{o}_i^t : Optimization Context.** Contains agent A_i 's additional, time-specific details (e.g., past performance or number of non-improving moves) that help adjust its strategy.

To effectively balance exploration and exploitation during the search, each agent is equipped with two specialized modules: an **improvement module** and an **exploration module**. A central component called the **router** dynamically decides which module to activate, depending on the current optimization context (see the center section of Figure 2). The improvement module applies a NI policy to refine the current solution, aiming to incrementally improve its quality. However, if the progress made by the NI policy stalls, the exploration module replaces the current solution with a new one via a NC policy. This new solution is generated based on a trade-off between quality and diversity, controlled by a conditioning weight (see the right side of Figure 2).

We elaborate on the functionalities and mechanisms of the modules and the router in the following sections. While we present our approach in the context of binary optimization problems, it is generalizable to other problem types. In Appendix B, we discuss how it can be adapted to permutation-based problems.

188 4.1 Improvement Module: Memory-based Neural Improvement Method

The memory-based NI policy, π_{NI} , refines solutions by taking an input $\mathbf{x}_i^{\text{impr}} = (\mathcal{I}, \mathbf{s}_i, \mathcal{M})$, consisting of the problem instance, agent i 's current solution \mathbf{s}_i , and shared memory information \mathcal{M} . It produces an action $a_i \in \mathcal{A}$ to improve the solution as follows:

$$\mathbf{s}'_i = \text{ApplyAction}(\mathbf{s}_i, a_i).$$

For binary problems, the `ApplyAction` function flips a specific bit. Formally, given a solution $\mathbf{s}_i = (s_{i1}, s_{i2}, \dots, s_{in}) \in \{0, 1\}^n$, action a_i corresponds to selecting an index $j \in \{1, \dots, n\}$, indicating the bit to flip. The updated solution \mathbf{s}'_i is thus:

$$s'_{ik} = \begin{cases} 1 - s_{ik}, & \text{if } k = j, \\ s_{ik}, & \text{otherwise.} \end{cases}$$

The **training** of the improvement policy employs a reward function with two components: an improvement reward and a repetition penalty.

The *improvement reward* captures the increase in the objective value of a candidate solution. Instead of assigning a reward for every action based on its immediate effect on the objective value, following

199 recent NI approaches [Barrett et al., 2020, Chalumeau et al., 2024], we use the best solution achieved
 200 by each agent, denoted as $\hat{\mathbf{s}}_i$, as a reference point. The improvement reward is only given when an
 201 agent discovers a solution that surpasses this baseline, and zero otherwise.

$$R_{\text{obj}}^i = \max[f(\mathbf{s}'_i), f(\hat{\mathbf{s}}_i)] - f(\hat{\mathbf{s}}_i). \quad (1)$$

202 This ensures that the cumulative reward that an agent receives throughout its entire trajectory
 203 corresponds to the total improvement in the objective value.

204 The *repetition penalty* discourages agents from visiting solutions already present in the shared memory
 205 \mathcal{M} . For agent A_i , the penalty is defined as:

$$R_{\text{rep}}^i = \begin{cases} -1 & \text{if } \mathbf{s}'_i \in \mathcal{M}, \\ 0 & \text{otherwise.} \end{cases} \quad (2)$$

206 The total reward is calculated as $R_{\text{NI}} = R_{\text{obj}}^i + w_{\text{rep}} \times R_{\text{rep}}^i$ where w_{rep} is the repetition penalty weight.
 207 For a complete description of the training methodology for the NI model, refer to Appendix C.

208 4.2 Exploration Module: Conditioned Networks for Balancing Quality and Diversity

209 The Exploration Module aims to prevent premature convergence by maintaining a diverse set of
 210 solutions in the population. To achieve this, we employ Conditioned Networks [Abels et al., 2019], a
 211 neural architecture originally developed for multi-objective reinforcement learning tasks [Felten et al.,
 212 2024]. Conditioned networks incorporate conditioning variables as context into their input, enabling
 213 the network to dynamically adjust its policy based on external parameters or specific objectives.

214 Specifically, we propose a conditioned Neural Constructive (cNC) policy π_{cNC} that, given an instance
 215 \mathcal{I} , a fixed subset of previously visited solutions $\mathcal{K} \subseteq \mathcal{M}$, and an exploration weight $\omega \in [0, 1]$ as part
 216 of its input, generates a new candidate solution balancing two competing goals: solution quality and
 217 diversity with respect to previously visited solutions. Here, ω directly modulates this balance, with
 218 higher values promoting exploration (generating more diverse solutions) and lower values favoring
 219 exploitation (producing higher-quality solutions).

220 We use a fixed-size subset \mathcal{K} instead of the dynamic memory to maintain consistent input dimensions
 221 and computational tractability. \mathcal{K} contains exactly the most recent solution from each agent, ensuring
 222 $|\mathcal{K}| = |\mathcal{A}|$.

223 Given input $\mathbf{x}_i^{\text{explor}} = (\mathcal{I}, \mathcal{K}, \omega)$, the policy π_{cNC} outputs a heatmap indicating preference scores for
 224 each item's inclusion. This heatmap is decoded into a solution using a Non-Autoregressive (NAR)
 225 approach [Joshi et al., 2020], which constructs the solution in a single step by greedily assigning
 226 the highest-valued choice for each item. Compared to autoregressive decoding, requiring $O(|V|)$
 227 sequential network evaluations, NAR decoding significantly reduces computational complexity to
 228 just a single forward pass, where $|V|$ is the number of items or nodes in the problem.

229 During **training**, the cNC model uses a bi-objective reward function that considers a linear combina-
 230 tion of quality and diversity rewards weighted by the condition weight ω used as input:

$$R_{\text{cNC}}(\mathbf{s}'_i) = (1 - \omega) \cdot f(\mathbf{s}'_i) + \omega \cdot \frac{1}{|\mathcal{K}|} \sum_{\mathbf{m} \in \mathcal{K}} d(\mathbf{s}', \mathbf{m}). \quad (3)$$

231 Here $f(\mathbf{s}'_i)$ is the objective value of the generated solution s'_i , and $d(\mathbf{s}'_i, \mathbf{m})$ is a distance metric
 232 measuring the dissimilarity between the new solution and the reference solution \mathbf{m} ¹.

233 Rather than uniformly sampling the exploration weight ω during different training episodes, we
 234 observed that focusing on extreme values (near 0 and 1) facilitates more effective learning of the
 235 Pareto front boundaries. Consequently, in each episode we sample ω from a Beta distribution with
 236 parameters $\alpha = \beta = 0.2$, which biases sampling towards these extreme values. The improved Pareto
 237 front achieved by the cNC model using this biased sampling is empirically validated in Appendix D.

238 During inference, we leverage the cNC model's ability to adjust the exploration weight using a
 239 cooling schedule based on the remaining execution budget. Specifically, for each iteration t out of a

¹We use the bitwise Hamming distance for binary solution vectors.

240 total budget T_{\max} , the exploration weight is defined as:

$$\omega(t) = \omega_{\text{start}} \left(1 - \frac{t}{T}\right)^{\phi} \quad (4)$$

241 where ω_{start} is the initial exploration weight and $\phi > 0$ is a cooling factor that controls the curvature
242 of the cooling schedule. We analyze the effect of different cooling schedules in the Appendix D.2.

243 4.3 Router

244 The Router dynamically assigns agents to either the Improvement Module or the Exploration Module
245 based on their performance.

246 By default, agents use the Improvement Module to refine their current solutions. To prevent stagnation,
247 the router monitors the number of consecutive iterations during which an agent fails to achieve an
248 improvement in its solution. If this count exceeds a predefined patience threshold (N_{patience}), the
249 Router redirects the agent to the Exploration Module to start the search from a new candidate solution.
250 We provide a detailed ablation study in Appendix E that systematically varies N_{patience} and analyzes
251 its impact on both solution quality and convergence.

252 To provide a comprehensive understanding of the interactions between the modules and the router,
253 we present the pseudo-code for MALOTE’s inference procedure in Appendix F.

254 4.4 Neural Network Architecture

255 Both the improvement policy π_{NI} and the exploration policy π_{cNC} are parameterized by Graph
256 Transformers (GT) [Dwivedi and Bresson, 2020], which ensure size- and permutation-invariance
257 through self-attention over graph-structured inputs. GT encodes node and edge features into latent
258 embeddings, which are decoded into policy-specific logits. For π_{NI} , the decoder outputs one logit per
259 node in V , indicating the probability of flipping each corresponding node. For π_{cNC} , it produces a
260 $|V| \times 2$ heatmap, assigning scores for class 0 or 1, which is greedily decoded into a solution. Detailed
261 hyperparameters and training configurations of the GT model are presented in Appendix G.

262 5 Experiments

263 We evaluate MALOTE on two benchmark problems, Maximum Cut (MC) [Dunning et al., 2018]
264 and Maximum Independent Set (MIS) [Lawler et al., 1980], with formal definitions and feature
265 processing details provided in Appendix A.

266 For each problem, we train the NI and cNC models on randomly generated Erdős–Rényi (ER) graphs
267 with a 15% edge probability and sizes ranging from 50 to 200 nodes. During inference, we use
268 a population size of $|A| = 20$ per instance, set a patience threshold of $N_{\text{patience}} = 500$ steps for
269 the router, and apply a linear cooling factor $\phi = 1$ for the exploration weight of the cNC model.
270 Additional parameters used for inference are provided in Appendix G.

271 Following recent studies [Ahn et al., 2020, Böther et al., 2021, Zhang et al., 2023], we assess
272 MALOTE’s generalization on larger ER graphs (700–800 nodes) and on more challenging RB
273 graphs [Xu and Li, 2000] (800–1200 nodes).

274 For a more comprehensive comparison, we include exact methods using the GUROBI solver [Gurobi
275 Optimization, LLC, 2023], greedy heuristics, metaheuristics such as Genetic Algorithms
276 (GA) [Kramer and Kramer, 2017] and Particle Swarm Optimization (PSO) [Kennedy and Eber-
277 hart, 1995], specialized algorithms like BURER [Burer et al., 2002] for MC and K_AMIS [Lamm et al.,
278 2016] for MIS, and learning-based methods including S2V-DQN [Khalil et al., 2017], ECO-DQN [Bar-
279 rett et al., 2020], FlowNet [Zhang et al., 2023], ANYCSP [Tönshoff et al., 2023], MARCO [Gar-
280 mendia et al., 2024] for MC, and additionally DGL [Böther et al., 2021], LwD [Ahn et al., 2020],
281 INTEL [Li et al., 2018] and DiffUCO [Sanokowski et al., 2024] for MIS. Together, these methods
282 span a broad spectrum of algorithms, including the state-of-the-art techniques. For full details on the
283 benchmark methods, see Appendix H.

284 Exact methods, heuristics, and metaheuristics have been executed using a cluster with 32 *Intel Xeon*
 285 X5650 CPUs. MALOTE and the other learning-based methods have been implemented using *PyTorch*
 286 2.0, and a *Nvidia H100* GPU has been used to train the models and perform inference².

Table 1: MC and MIS performance table. The best overall results are highlighted in bold. *Used to compute the ratios.

	Method	Type	ER700-800			RB800-1200		
			Objective ↑	Ratio ↑	Time ↓	Objective ↑	Ratio ↑	Time ↓
Maximum Cut (MC)	GUROBI	Exact	24048.93	0.992	10m	23729.44	0.747	10m
	Greedy	Heuristic	23774.79	0.980	0.03s	30619.32	0.964	0.04s
	GA	Metaheuristic	24211.64	0.999	1m	31762.89	1.000	1m
	PSO	Metaheuristic	24201.78	0.999	1m	31764.80*	1.000	1m
	BURER	Specialized	24235.93*	1.000	1m	29791.52	0.938	1m
	S2V-DQN	RL / NC	21581.79	0.890	10.1s	22014.93	0.693	13.4s
Maximum Independent Set (MIS)	FlowNet	UL / NC	21727.19	0.896	2.25m	23410.60	0.785	2.97m
	ECO-DQN	RL / NI	24114.06	0.994	2.10m	29638.78	0.933	3.00m
	ANYCSP	RL / NI	24211.00	0.999	35.7m	31544.76	0.993	42.4m
	MARCO	RL / NI	24205.97	0.998	1.67m	29780.71	0.938	2.75m
	cNC	RL / NC	23394.25	0.965	0.01s	18405.78	0.579	0.01s
	MALOTE _s	RL / NI + cNC	24231.19	1.000	30s	31766.79	1.000	30s
	MALOTE	RL / NI + cNC	24238.82	1.000	5m	31767.55	1.000	5m
Maximum Cut (MC)	GUROBI	Exact	43.64	0.970	10m	41.34	0.957	10m
	Greedy	Heuristic	38.85	0.863	0.05s	37.78	0.875	0.06s
	GA	Metaheuristic	43.97	0.977	1m	41.39	0.959	1m
	PSO	Metaheuristic	43.69	0.971	1m	41.19	0.955	1m
	KAMIS	Specialized	44.98*	1.000	1m	43.15*	1.000	1m
	DGL	SL / Hybrid	38.71	0.861	11s	32.32	0.750	2.61s
Maximum Independent Set (MIS)	INTEL	SL / Hybrid	41.13	0.913	10s	34.24	0.794	2.44s
	LwD	RL / NI	41.17	0.915	4s	34.50	0.799	0.86s
	FlowNet	UL / NC	41.14	0.914	2s	37.48	0.868	0.46s
	DiffUCO	UL / NC	42.21	0.938	2.6s	38.87	0.900	0.42s
	MARCO	RL / NI	43.78	0.973	17s	40.13	0.930	6s
	cNC	RL / NC	38.96	0.866	0.03s	35.39	0.820	0.04s
Maximum Cut (MC)	MALOTE _s	RL / NI + cNC	44.96	1.000	30s	39.97	0.926	30s
	MALOTE	RL / NI + cNC	45.38	1.009	5m	40.97	0.949	5m

287 5.1 Performance Experiments

288 We evaluate our framework using three key metrics: the average objective value $f(\mathbf{s})$ over the entire
 289 dataset, the performance ratio $R(\mathbf{s}) = \frac{f(\mathbf{s})}{f_{\text{best}}}$, where f_{best} represents the best known objective value for
 290 the instance, and the average execution time per instance.

291 In this first experiment, we aim to showcase the best possible performance of each method by setting
 292 time or iteration limits tailored to their design. Exact methods, such as Gurobi, are allowed 10 minutes
 293 to find high-quality solutions. Heuristics run until they reach their final solution. Metaheuristics and
 294 specialized algorithms run for 1 minute per each instance. Learning-based baselines follow the limits
 295 and setups proposed in their original papers. Our proposed method, MALOTE, is evaluated with a
 296 short 30-second run (MALOTE_s), and a longer time limit of 5-minutes (MALOTE).

297 As shown in Table 1, MALOTE outperforms all evaluated methods on the MC-ER, MC-RB, and
 298 MIS-ER benchmarks, and achieves the best performance among learning-based approaches across
 299 all four benchmarks. Notably, our standalone cNC policy, run with the exploration weight set to 0,
 300 achieves reasonable performance in a single inference pass, offering a remarkably fast alternative to
 301 traditional greedy heuristics.

302 Regarding computational time, it is important to note that CPU vs. GPU runtimes are not directly
 303 comparable. While we include average runtime primarily to provide a coarse view of computational
 304 cost, our focus is on solution quality and anytime performance. In some experiments, MALOTE is
 305 given a larger time budget than certain baselines, mainly because it had not yet converged to its best

²The source code, along with all scripts necessary to reproduce the experimental results presented in this paper, will be made publicly available upon manuscript acceptance.

306 solution. However, as we will demonstrate in the following experiment, MALOTE still outperforms
 307 these baselines even when given a substantially shorter execution time.

308 5.2 Anytime performance

309 While MALOTE performs strongly under the proposed time limits (5 minutes and 30 seconds), it is
 310 also important to assess its behavior under varying time budgets, that is, its anytime performance. To
 311 this end, Figure 3 shows the best objective values obtained over time across different benchmarks.
 312 The results demonstrate that MALOTE consistently delivers superior solution quality compared to all
 313 evaluated baselines across all MC datasets and on ER graphs in the MIS problem.

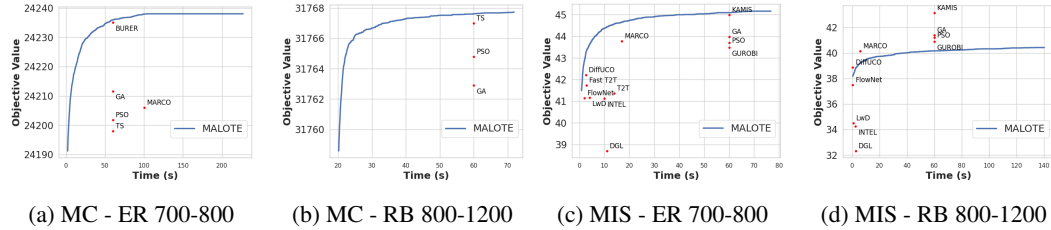


Figure 3: Anytime performance of MALOTE and baselines.

314 **Additional Experiments** In Appendix J, we compare MALOTE against equivalent metaheuristics,
 315 such as Genetic Algorithms (GA) and Particle Swarm Optimization (PSO), under varying time
 316 budgets. The impact of centralized memory during training is analyzed in Appendix I. Lastly, ablation
 317 studies on MALOTE, along with their corresponding anytime performance curves, are reported in
 318 Appendix J.1.

319 6 Conclusions

320 In this paper, we introduced **MALOTE**, a multi-agent reinforcement learning framework that balances
 321 exploration and exploitation for robust anytime performance. By combining multiple agents, each
 322 with exploration and improvement modules, and a centralized memory, MALOTE fosters diversity
 323 and mitigates premature convergence. Experiments on Maximum Cut and Maximum Independent Set
 324 confirm its ability to steadily improve solutions with extended computational budgets, outperforming
 325 state-of-the-art methods on three of four evaluated benchmarks.

326 **Limitations and Future Work** While MALOTE demonstrates promising results, there are numerous
 327 opportunities for future investigation. One limitation comes from the information loss incurred
 328 when the cNC policy considers only a subset of visited solutions. This sub-sampling discards potentially
 329 valuable information about the search history. Future work could explore methods to mitigate
 330 this information loss, such as developing techniques to aggregate or summarize the dynamically
 331 changing information of past visited solutions, perhaps through learned embeddings or more sophis-
 332 ticated memory structures. Another area for improvement lies in the control flow between the
 333 exploration and improvement modules. Currently, the routing strategy that determines when to ex-
 334 ecute each module is relatively simple. Exploring more intelligent and adaptive routing strategies could
 335 further refine performance and potentially reduce unnecessary computation by dynamically routing
 336 to each module based on the current state of the search. Finally, it would be particularly interesting
 337 to explore the use of the conditioned Neural Constructive policy in multi-objective combinatorial
 338 optimization problems, where balancing competing objectives could further highlight its strengths.

339 References

- 340 Axel Abels, Diederik Roijers, Tom Lenaerts, Ann Nowé, and Denis Steckelmacher. Dynamic weights in
 341 multi-objective deep reinforcement learning. In *International conference on machine learning*, pages 11–20.
 342 PMLR, 2019.
- 343 Sungsoo Ahn, Younggyo Seo, and Jinwoo Shin. Learning what to defer for maximum independent sets. In
 344 *International conference on machine learning*, pages 134–144. PMLR, 2020.

- 345 Stefano V Albrecht, Filippos Christianos, and Lukas Schäfer. *Multi-agent reinforcement learning: Foundations*
346 and modern approaches. MIT Press, 2024.
- 347 Thomas Barrett, William Clements, Jakob Foerster, and Alex Lvovsky. Exploratory combinatorial optimization
348 with reinforcement learning. In *Proceedings of the AAAI conference on artificial intelligence*, volume 34,
349 pages 3243–3250, 2020.
- 350 Thomas D Barrett, Christopher WF Parsonson, and Alexandre Laterre. Learning to solve combinatorial graph
351 partitioning problems via efficient exploration. *arXiv preprint arXiv:2205.14105*, 2022.
- 352 Julien Baste, Michael R Fellows, Lars Jaffke, Tomáš Masařík, Mateus de Oliveira Oliveira, Geevarghese Philip,
353 and Frances A Rosamond. Diversity of solutions: An exploration through the lens of fixed-parameter
354 tractability theory. *Artificial Intelligence*, 303:103644, 2022.
- 355 Irwan Bello, Hieu Pham, Quoc V Le, Mohammad Norouzi, and Samy Bengio. Neural combinatorial optimization
356 with reinforcement learning. *arXiv preprint arXiv:1611.09940*, 2016.
- 357 Yoshua Bengio, Andrea Lodi, and Antoine Prouvost. Machine learning for combinatorial optimization: a
358 methodological tour d’horizon. *European Journal of Operational Research*, 290(2):405–421, 2021.
- 359 Christian Blum and Andrea Roli. Metaheuristics in combinatorial optimization: Overview and conceptual
360 comparison. *ACM computing surveys (CSUR)*, 35(3):268–308, 2003.
- 361 Mohammad Reza Bonyadi and Zbigniew Michalewicz. Particle swarm optimization for single objective
362 continuous space problems: a review. *Evolutionary computation*, 25(1):1–54, 2017.
- 363 Maximilian Böther, Otto Kißig, Martin Taraz, Sarel Cohen, Karen Seidel, and Tobias Friedrich. What’s wrong
364 with deep learning in tree search for combinatorial optimization. In *International Conference on Learning
365 Representations*, 2021.
- 366 Xavier Bresson and Thomas Laurent. The transformer network for the traveling salesman problem. *arXiv
367 preprint arXiv:2103.03012*, 2021.
- 368 Samuel Burer, Renato DC Monteiro, and Yin Zhang. Rank-two relaxation heuristics for max-cut and other
369 binary quadratic programs. *SIAM Journal on Optimization*, 12(2):503–521, 2002.
- 370 Lucian Busoni, Robert Babuska, and Bart De Schutter. A comprehensive survey of multiagent reinforcement
371 learning. *IEEE Transactions on Systems, Man, and Cybernetics, Part C (Applications and Reviews)*, 38(2):
372 156–172, 2008.
- 373 Quentin Cappart, Didier Chételat, Elias B Khalil, Andrea Lodi, Christopher Morris, and Petar Veličković.
374 Combinatorial optimization and reasoning with graph neural networks. *Journal of Machine Learning
375 Research*, 24(130):1–61, 2023.
- 376 Felix Chalumeau, Refiloe Shabe, Noah De Nicola, Arnu Pretorius, Thomas D Barrett, and Nathan Grinsztajn.
377 Memory-enhanced neural solvers for efficient adaptation in combinatorial optimization. *arXiv preprint
378 arXiv:2406.16424*, 2024.
- 379 Xinyun Chen and Yuandong Tian. Learning to perform local rewriting for combinatorial optimization. *Advances
380 in Neural Information Processing Systems*, 32, 2019.
- 381 Paulo Roberto de O da Costa, Jason Rhuggenaath, Yingqian Zhang, and Alp Akcay. Learning 2-opt heuristics
382 for the traveling salesman problem via deep reinforcement learning. In *Asian conference on machine learning*,
383 pages 465–480. PMLR, 2020.
- 384 Marco Dorigo and Thomas Stützle. *Ant colony optimization: overview and recent advances*. Springer, 2019.
- 385 Iain Dunning, Swati Gupta, and John Silberholz. What works best when? a systematic evaluation of heuristics
386 for max-cut and qubo. *INFORMS Journal on Computing*, 30(3):608–624, 2018.
- 387 Vijay Prakash Dwivedi and Xavier Bresson. A generalization of transformer networks to graphs. *arXiv preprint
388 arXiv:2012.09699*, 2020.
- 389 Florian Felten, El-Ghazali Talbi, and Grégoire Danoy. Multi-objective reinforcement learning based on decom-
390 position: A taxonomy and framework. *Journal of Artificial Intelligence Research*, 79:679–723, 2024.
- 391 Andoni I Garmendia, Josu Ceberio, and Alexander Mendiburu. Neural improvement heuristics for graph
392 combinatorial optimization problems. *IEEE Transactions on Neural Networks and Learning Systems*, 2023.

- 393 Andoni I Garmendia, Quentin Cappart, Josu Ceberio, and Alexander Mendiburu. Marco: a memory-augmented
 394 reinforcement framework for combinatorial optimization. In *Proceedings of the Thirty-Third International*
 395 *Joint Conference on Artificial Intelligence*, pages 6931–6939, 2024.
- 396 Fred Glover. Tabu search: A tutorial. *Interfaces*, 20(4):74–94, 1990.
- 397 Nathan Grinsztajn, Daniel Furelos-Blanco, Shikha Surana, Clément Bonnet, and Tom Barrett. Winner takes
 398 it all: Training performant rl populations for combinatorial optimization. *Advances in Neural Information*
 399 *Processing Systems*, 36:48485–48509, 2023.
- 400 Gurobi Optimization, LLC. Gurobi Optimizer Reference Manual, 2023. URL <https://www.gurobi.com>.
- 401 André Hottung and Kevin Tierney. Neural large neighborhood search for the capacitated vehicle routing problem.
 402 In *ECAI 2020*, pages 443–450. IOS Press, 2020.
- 403 André Hottung, Mridul Mahajan, and Kevin Tierney. Polynet: Learning diverse solution strategies for neural
 404 combinatorial optimization. *arXiv preprint arXiv:2402.14048*, 2024.
- 405 Jorik Jooken, Pieter Leyman, Tony Wauters, and Patrick De Causmaecker. Exploring search space trees using an
 406 adapted version of monte carlo tree search for combinatorial optimization problems. *Computers & Operations*
 407 *Research*, 150:106070, 2023.
- 408 Chaitanya K Joshi, Quentin Cappart, Louis-Martin Rousseau, and Thomas Laurent. Learning the travelling
 409 salesperson problem requires rethinking generalization. *arXiv preprint arXiv:2006.07054*, 2020.
- 410 James Kennedy and Russell Eberhart. Particle swarm optimization. In *Proceedings of ICNN'95-international*
 411 *conference on neural networks*, volume 4, pages 1942–1948. ieee, 1995.
- 412 Elias Khalil, Hanjun Dai, Yuyu Zhang, Bistra Dilkina, and Le Song. Learning combinatorial optimization
 413 algorithms over graphs. *Advances in neural information processing systems*, 30, 2017.
- 414 Scott Kirkpatrick, C Daniel Gelatt Jr, and Mario P Vecchi. Optimization by simulated annealing. *science*, 220
 415 (4598):671–680, 1983.
- 416 Wouter Kool, Herke van Hoof, and Max Welling. Attention, learn to solve routing problems! In *International*
 417 *Conference on Learning Representations*, 2018.
- 418 Oliver Kramer and Oliver Kramer. *Genetic algorithms*. Springer, 2017.
- 419 Yeong-Dae Kwon, Jinho Choo, Byoungjip Kim, Iljoo Yoon, Youngjune Gwon, and Seungjai Min. Pomo: Policy
 420 optimization with multiple optima for reinforcement learning. *Advances in Neural Information Processing*
 421 *Systems*, 33:21188–21198, 2020.
- 422 Sebastian Lamm, Peter Sanders, Christian Schulz, Darren Strash, and Renato F Werneck. Finding near-optimal
 423 independent sets at scale. In *2016 Proceedings of the Eighteenth Workshop on Algorithm Engineering and*
 424 *Experiments (ALENEX)*, pages 138–150. SIAM, 2016.
- 425 Eugene L. Lawler, Jan Karel Lenstra, and AHG Rinnooy Kan. Generating all maximal independent sets:
 426 Np-hardness and polynomial-time algorithms. *SIAM Journal on Computing*, 9(3):558–565, 1980.
- 427 Zhuwen Li, Qifeng Chen, and Vladlen Koltun. Combinatorial optimization with graph convolutional networks
 428 and guided tree search. *Advances in neural information processing systems*, 31, 2018.
- 429 Hao Lu, Xingwen Zhang, and Shuang Yang. A learning-based iterative method for solving vehicle routing
 430 problems. In *International conference on learning representations*, 2019.
- 431 Fu Luo, Xi Lin, Zhenkun Wang, Xialiang Tong, Mingxuan Yuan, and Qingfu Zhang. Self-improved learning for
 432 scalable neural combinatorial optimization. *arXiv preprint arXiv:2403.19561*, 2024.
- 433 Nina Mazyavkina, Sergey Sviridov, Sergei Ivanov, and Evgeny Burnaev. Reinforcement learning for combinatorial
 434 optimization: A survey. *Computers & Operations Research*, 134:105400, 2021.
- 435 Melanie Mitchell. *An introduction to genetic algorithms*. MIT press, 1998.
- 436 Sajad Modaresi, Denis Sauré, and Juan Pablo Vielma. Learning in combinatorial optimization: What and how to
 437 explore. *Operations Research*, 68(5):1585–1604, 2020.
- 438 Ankur Nath and Alan Kuhnle. A benchmark for maximum cut: Towards standardization of the evaluation of
 439 learned heuristics for combinatorial optimization. *arXiv preprint arXiv:2406.11897*, 2024.

- 440 Shengjie Ren, Zhijia Qiu, Chao Bian, Miqing Li, and Chao Qian. Maintaining diversity provably helps in
441 evolutionary multimodal optimization. *arXiv preprint arXiv:2406.02658*, 2024.
- 442 Sebastian Sanokowski, Sepp Hochreiter, and Sebastian Lehner. A diffusion model framework for unsupervised
443 neural combinatorial optimization. *arXiv preprint arXiv:2406.01661*, 2024.
- 444 Jiwoo Son, Zhikai Zhao, Federico Berto, Chuanbo Hua, Changhyun Kwon, and Jinkyoo Park. Neural combina-
445 torial optimization for real-world routing. *arXiv preprint arXiv:2503.16159*, 2025.
- 446 Haoran Sun, Katayoon Goshvadi, Azade Nova, Dale Schuurmans, and Hanjun Dai. Revisiting sampling for
447 combinatorial optimization. In *International Conference on Machine Learning*, pages 32859–32874. PMLR,
448 2023.
- 449 Rui Sun, Zhi Zheng, and Zhenkun Wang. Learning encodings for constructive neural combinatorial optimization
450 needs to regret. In *Proceedings of the AAAI Conference on Artificial Intelligence*, volume 38, pages 20803–
451 20811, 2024.
- 452 Zhiqing Sun and Yiming Yang. Difusco: Graph-based diffusion solvers for combinatorial optimization. *Advances*
453 *in neural information processing systems*, 36:3706–3731, 2023.
- 454 Jan Tönshoff, Berke Kisim, Jakob Lindner, and Martin Grohe. One model, any csp: graph neural networks as
455 fast global search heuristics for constraint satisfaction. In *Proceedings of the Thirty-Second International*
456 *Joint Conference on Artificial Intelligence*, pages 4280–4288, 2023.
- 457 Ashish Vaswani, Noam Shazeer, Niki Parmar, Jakob Uszkoreit, Llion Jones, Aidan N Gomez, Łukasz Kaiser,
458 and Illia Polosukhin. Attention is all you need. *Advances in neural information processing systems*, 30, 2017.
- 459 Oriol Vinyals, Meire Fortunato, and Navdeep Jaitly. Pointer networks. *Advances in neural information processing*
460 *systems*, 28, 2015.
- 461 Ronald J Williams. Simple statistical gradient-following algorithms for connectionist reinforcement learning.
462 *Machine learning*, 8:229–256, 1992.
- 463 Yaxin Wu, Wen Song, Zhiguang Cao, Jie Zhang, and Andrew Lim. Learning improvement heuristics for
464 solving routing problems. *IEEE transactions on neural networks and learning systems*, 33(9):5057–5069,
465 2021.
- 466 Ke Xu and Wei Li. Exact phase transitions in random constraint satisfaction problems. *Journal of Artificial*
467 *Intelligence Research*, 12:93–103, 2000.
- 468 Haoran Ye, Jiarui Wang, Zhiguang Cao, Helan Liang, and Yong Li. Deepaco: neural-enhanced ant systems for
469 combinatorial optimization. *Advances in Neural Information Processing Systems*, 36, 2024.
- 470 Cong Zhang, Wen Song, Zhiguang Cao, Jie Zhang, Puay Siew Tan, and Xu Chi. Learning to dispatch for job
471 shop scheduling via deep reinforcement learning. *Advances in neural information processing systems*, 33:
472 1621–1632, 2020.
- 473 Dinghuai Zhang, Hanjun Dai, Nikolay Malkin, Aaron Courville, Yoshua Bengio, and Ling Pan. Let the flows tell:
474 Solving graph combinatorial problems with gflownets. In *Thirty-seventh Conference on Neural Information*
475 *Processing Systems*, 2023.
- 476 Changliang Zhou, Xi Lin, Zhenkun Wang, Xialiang Tong, Mingxuan Yuan, and Qingfu Zhang. Instance-
477 conditioned adaptation for large-scale generalization of neural combinatorial optimization. *arXiv preprint*
478 *arXiv:2405.01906*, 2024.

479 **A Application to the Maximum Cut and Maximum Independent Set**

480 In this study, we address two fundamental graph-based combinatorial optimization problems: Maximum
 481 Cut (MC) [Dunning et al., 2018] and Maximum Independent Set (MIS) [Lawler et al., 1980].
 482 Both problems are defined on an undirected graph $G = (V, E)$, where V represents the set of nodes
 483 and E denotes the set of edges.

484 **A.1 Maximum Cut (MC)**

485 The Maximum Cut problem seeks to partition the node set V into two disjoint subsets V_1 and V_2
 486 such that the number of edges between these subsets, known as the cut size, is maximized. Formally,
 487 given a binary solution vector $\mathbf{s} \in \{0, 1\}^{|V|}$, where $s_u = 0$ if node u is assigned to V_1 and $s_u = 1$ if
 488 assigned to V_2 , the objective function can be expressed as:

$$\max_{\mathbf{s}} \sum_{(u,v) \in E} \delta(s_u \neq s_v), \quad (5)$$

489 where $\delta(\cdot)$ is the Kronecker delta function, which equals 1 if its argument is true and 0 otherwise.

490 **A.2 Maximum Independent Set (MIS)**

491 The Maximum Independent Set problem aims to identify the largest possible subset of nodes $S \subseteq V$
 492 such that no two nodes in S are adjacent; that is, $(u, v) \notin E$ for all $u, v \in S$. Formally, given a binary
 493 solution vector $\mathbf{s} \in \{0, 1\}^{|V|}$, where $s_u = 1$ if node u is included in the independent set and $s_u = 0$
 494 otherwise, the objective function can be formulated as:

$$\max_{\mathbf{s}} \sum_{u \in V} s_u \quad \text{subject to} \quad s_u + s_v \leq 1 \quad \forall (u, v) \in E. \quad (6)$$

495 **A.3 Feature Encoding**

496 As discussed in Section 4, both the NI and cNC policies rely on node and edge features to iteratively
 497 modify or construct a solution, respectively. These features capture information from the problem
 498 instance, the current solution (in the case of NI), a set of reference solutions stored in memory, or a
 499 conditioning value (used by cNC).

500 For both MC and MIS, **instance information** is derived from the graph’s adjacency matrix (and
 501 optionally, edge weights). This structure is encoded as edge features, where each edge is represented
 502 by a binary vector using a one-hot encoding scheme to indicate the presence or absence of a connection
 503 between node pairs.

504 In binary problems like MC and MIS, a **solution** can be naturally represented as a binary node feature
 505 vector, assigning each node a feature value of 0 or 1. To encode **memory information** in the NI
 506 policy, we follow the approach of Garmendia et al. [2024], where the k nearest solutions in memory
 507 \mathcal{M} , measured by their similarity to the current solution, are selected and aggregated. Similarity is
 508 computed by the inner product $\langle \mathbf{s}, \mathbf{s}_i \rangle$ between the current solution \mathbf{s} and each solution $\mathbf{s}_i \in \mathcal{M}$. The
 509 resulting aggregation is a weighted average over the k selected solutions, producing a continuous
 510 node feature vector of dimension $|V|$, which serves as an additional input to the NI policy.

511 In the cNC policy, the fixed set of reference solutions \mathcal{K} is encoded by assigning one feature dimension
 512 per solution $\mathbf{s}_i \in \mathcal{K}$. Thus, the reference set contributes $|\mathcal{K}|$ additional node features. Additionally,
 513 the conditioning parameter, or exploration weight ω , is appended as a constant scalar feature to each
 514 node, providing one more node feature dimension.

515 In terms of feature breakdown:

- 516 • **NI policy:** Each edge is assigned one feature to represent the problem instance (e.g., edge
 517 presence or weight). Each node receives two features: one from the current solution (a
 518 binary value) and another from the aggregated memory information.
- 519 • **cNC policy:** Each edge also has one instance-based feature. Each node receives $|\mathcal{K}|$ features
 520 from the reference solutions, plus one feature for the exploration weight, resulting in a total
 521 of $|\mathcal{K}| + 1$ node features.

522 **A.3.1 Exploiting Symmetries**

523 Exploiting the symmetry in the MC problem, where inverting all node assignments yields solutions
524 with identical objective values, we introduce a specific encoding strategy for the cNC model. We
525 preset the first node to a fixed set (e.g., value = 1) to establish a reference point. Additionally, we
526 assign a learnable parameter to this first node and a separate learnable parameter to the remaining
527 nodes, to allow the model to recognize the reference node.

528 **B Application of MALOTE to Alternative Problems**

529 To adapt MALOTE to a new combinatorial optimization problem, three key components must be
530 addressed:

531 **Input Feature Representation.** The first step involves defining suitable node and edge features
532 specific to the problem at hand. These features encode the structure and constraints of the problem
533 instance. Once defined, they are processed by the encoder—such as the Graph Transformer (GT)
534 architecture used in this work (detailed in Appendix G)—to produce node (and optionally edge)
535 embeddings.

536 **Action Mapping.** The second step requires adapting how these embeddings are used to take actions.
537 In the case of NI, this means modifying a current solution based on the embeddings. For the cNC
538 policy, this entails constructing new solutions from scratch using the embeddings and the current
539 exploration weight.

540 **Memory and Similarity Integration.** Finally, integrating the shared memory component involves
541 defining a suitable representation for storing solutions and designing a problem-specific similarity
542 metric to retrieve the k -nearest neighbors. These metrics are also used to condition the cNC policy
543 during training and inference.

544 In the following, we illustrate how these three components can be instantiated for three representative
545 problems: the Traveling Salesman Problem (TSP), the Knapsack Problem (KP), and the Job-Shop
546 Scheduling Problem (JSSP).

547 **B.1 Graph Features in Alternative Problems**

548 The formulation of node and edge features varies depending on the problem domain.

549 In the TSP, node features can be defined using the spatial coordinates of the cities, while edge features
550 typically represent the distances between city pairs.

551 In the KP, nodes correspond to items, with their primary node feature being the item’s weight. The
552 total knapsack capacity can either be appended as a global scalar feature to each node or, alternatively,
553 item weights can be normalized by the knapsack capacity to reflect their relative contribution.

554 The JSSP presents a more complex structure, as it involves two distinct entities: jobs and machines.
555 A natural representation is to use a heterogeneous graph, where each node corresponds to either a job
556 or a machine. Node features should therefore include an indicator denoting the type of node (job or
557 machine). Edge features are used to encode processing times: an edge from job node i to machine
558 node j carries the processing time required for job i on machine j , if such an operation is defined.

559 **B.2 Actions in Alternative Problems**

560 Defining actions varies significantly depending on the type of policy: NI or cNC, and the nature of
561 the problem.

562 In TSP and other permutation-based problems, NI actions correspond to modifications of the current
563 permutation of nodes. These include common local operators such as swap, insertion, or 2-opt, all of
564 which can be represented by a pair of nodes (i.e., an edge). Consequently, it is advantageous to use
565 edge embeddings, allowing the decoder to output edge logits. At each step, a probability distribution
566 over edges defines the likelihood of each possible modification.

567 In the cNC setting for TSP, solutions are typically constructed greedily using edge-based heatmaps,
 568 as in non-autoregressive (NAR) decoding frameworks [Joshi et al., 2020], where edges are scored
 569 and selected sequentially to form a valid tour.
 570 For the KP, NI actions involve adding or removing individual items from the current solution. In
 571 contrast, cNC policies apply node-level heatmaps to construct solutions directly in a single pass,
 572 where the selection probabilities are derived from node embeddings.
 573 In the JSSP, actions must respect the precedence and machine constraints that govern feasible
 574 schedules. For NI policies, actions correspond to local rescheduling moves, such as swapping the
 575 execution order of two operations on the same machine or shifting an operation earlier or later in
 576 time within its machine queue. These actions can be encoded as edges between operation nodes on
 577 the same machine, and thus, similar to TSP, edge embeddings and logits can be used to select the
 578 next local modification.
 579 In cNC, the construction process involves assigning operations to time slots in a way that respects
 580 both job precedence and machine availability. A natural approach is to define a greedy NAR decoding
 581 process, where the model outputs a heatmap over possible job-machine-time triplets. At each
 582 decoding step, the highest-scoring operation is scheduled next, progressively constructing a valid
 583 schedule until all operations are placed.

584 B.3 Similarity Measures

585 In the TSP, a convenient way to represent visited solutions is by storing the set of edges that belong
 586 to those tours, via a one-hot encoding in edge features. Regarding the similarity between solutions,
 587 permutation-based distance metrics could be used, such as Kendall Tau, or Cayley distance.
 588 In the KP, solutions are binary vectors indicating whether each item is included (1) or excluded (0)
 589 from the knapsack, and thus, can be represented as node features. The binary format of solutions
 590 is naturally suited to Hamming distance, which counts the number of differing bits between two
 591 solutions.
 592 For the JSSP, there are multiple alternatives: one is to encode solutions as a vector of operation start
 593 times, and compute similarity using Euclidean distance or mean absolute error between these vectors.
 594 Another option is to represent solutions as a sequence of operation-machine assignments and use
 595 sequence-based metrics such as Kendall Tau or edit distance to compare them.

596 C Training Details of the Improvement Module

597 This section details the training procedure for the NI model within the improvement module. The
 598 training process consists of multiple episodes, each involving a batch of randomly generated problem
 599 instances. For each instance in the batch, a set of agents \mathcal{A} is initialized, each agent A_i starting with a
 600 candidate solution s_i^0 and a centralized memory \mathcal{M} shared by the agents.
 601 Each episode proceeds through T optimization steps. In each step t , every agent proposes a modifi-
 602 cation to its current candidate solution based on the problem instance, its current solution, and the
 603 shared memory. After applying the proposed modification, rewards R_i^t are computed according to
 604 Equations 1 and 2, and the updated solutions are stored in the memory.
 605 At the end of each episode, the parameters of the NI model are updated using the REINFORCE
 606 algorithm [Williams, 1992], maximizing the expected cumulative reward across all agents over T
 607 steps. The objective can be formally defined as:

$$\mathcal{J}(\boldsymbol{\theta}) = \mathbb{E}_{\pi_{\boldsymbol{\theta}}} \left[\sum_{i=1}^{|\mathcal{A}|} \sum_{t=0}^{T-1} \gamma^t R_i^t \right], \quad (7)$$

608 where $\pi_{\boldsymbol{\theta}}$ denotes the joint policy of all agents, parameterized by $\boldsymbol{\theta}$, $|\mathcal{A}|$ is the number of agents or
 609 the population size, and γ is the discount factor that prioritizes immediate rewards over distant ones.

Algorithm 1 NI - Training Procedure

Input: Distribution of instances \mathcal{D} , population size $|\mathcal{A}|$, number of training episodes E , episode length T , NI policy π with parameters θ

Training:

Initialize policy network π_θ

for episode $e = 1$ to E **do**

$\mathcal{I} \leftarrow$ Sample a batch of M problem instances from \mathcal{D}

for each instance m in the batch **do**

Initialize:

for each Agent $i \in \mathcal{A}$ **do**

$s_i^0 \leftarrow$ RandomInitialization()

end for

Initialize shared memory $\mathcal{M}_0 \leftarrow \emptyset$

Main loop:

for $t = 0$ to $T - 1$ **do**

for each Agent $i \in \mathcal{A}$ **do**

$x_i^t \leftarrow (\mathcal{I}, s_i^t, \mathcal{M}_t)$

$a_i^t \sim \pi_\theta(\cdot | x_i^t)$

$s_i^{t+1} \leftarrow$ ApplyAction(s_i^t, a_i^t)

$R_i^t \leftarrow R_{\text{obj}} + w_{\text{rep}} \cdot R_{\text{rep}}$

$\mathcal{M}_{t+1} \leftarrow$ UpdateMemory(\mathcal{M}_t, s_i^{t+1})

end for

end for

end for

Policy Update:

$b \leftarrow \frac{1}{|\mathcal{A}|} \sum_{i=1}^{|\mathcal{A}|} \sum_{t=1}^T R_i^t \quad \{\text{baseline}\}$

$A_i^t \leftarrow \left(\sum_{k=0}^{T-t} \gamma^k R_i^{t+k} \right) - b \quad \{\text{advantage}\}$

$\Delta\theta \leftarrow \eta \sum_{i=1}^{|\mathcal{A}|} \sum_{t=0}^{T-1} \nabla_\theta \log \pi_\theta(a_i^t | x_i^t) \cdot A_i^t.$

$\theta \leftarrow \theta + \Delta\theta$

end for

Output: Trained policy parameters θ

- 610 To reduce the variance of the gradient estimator, a baseline strategy is usually adopted. Specifically,
 611 the average reward across all agents within the episode is used as the baseline:

$$b = \frac{1}{|\mathcal{A}|} \sum_{i=1}^{|\mathcal{A}|} \sum_{t=0}^{T-1} R_i^t. \quad (8)$$

- 612 The advantage for each agent i at each step t is then computed as:

$$A_i^t = \left(\sum_{k=0}^{T-t-1} \gamma^k R_i^{t+k} \right) - b. \quad (9)$$

- 613 The policy parameters are updated using the REINFORCE gradient:

$$\nabla_\theta \mathcal{J}(\theta) \approx \sum_{i=1}^{|\mathcal{A}|} \sum_{t=0}^{T-1} \nabla_\theta \log \pi_\theta(a_i^t | x_i^t) \cdot A_i^t. \quad (10)$$

- 614 The complete training procedure is outlined in Algorithm 1. For clarity, we omit the batch size
 615 summation in the parameter update calculations within the algorithm.

616 **C.1 Training Hyperparameters**

- 617 Table 2 presents the training hyperparameters used. To promote generalization to different graph
 618 sizes, we vary the size of the generated instances across episodes. Specifically, the number of nodes
 619 for each instance is sampled uniformly in the range [50, 200].

Table 2: Used Training Hyperparameters.

Hyperparameter	Value
Episodes	100k
Min Problem Size	50
Max Problem Size	200
Batch Size	128
Population Size	5
Episode Length T	3
γ (Discount)	0.95
Optimizer	AdamW
Learning Rate η	5×10^{-5}
Betas (AdamW)	(0.9, 0.95)
Weight Decay (AdamW)	0.1
Memory Type	Marco-shared
Random Seed	42

620 D Conditioned Neural Constructive

621 The conditioned Neural Constructive (cNC) offers significant advantages over training multiple
 622 independent models for varying exploration preferences. Instead of discretizing the preference space
 623 and training a separate model for each discrete value, cNC learns a continuous function conditioned
 624 on the exploration weight. This approach has several key benefits: (1) it requires training only a
 625 single model; and (2) it allows for fine-grained control over the exploration-exploitation balance by
 626 sampling any value within the continuous preference range.

627 However, training a cNC requires careful consideration of the training process. In each training
 628 episode, a batch of random problem instances is initialized along with a set of diverse candidate
 629 solutions. These solutions are used as reference to encourage the generation of distinct and high-
 630 quality solutions. Additionally, a random exploration weight is sampled from the range [0, 1] in
 631 each episode, providing the conditioning signal for the network. This stochastic sampling of the
 632 exploration weight is essential for the cNC to learn a robust mapping between exploration preference
 633 and constructive behavior.

634 The cNC policy is trained using the REINFORCE algorithm, following the same procedure as the NI
 635 policy described in Appendix C. The main distinction lies in the baseline computation: rather than
 636 aggregating rewards from multiple agents, the cNC training performs multiple rollouts (i.e., NAR
 637 decoding of solutions) for each instance, and uses the average reward across these rollouts as the
 638 baseline.

639 The general training process is outlined in Algorithm 2. For training the cNC in this work, we
 640 used a batch of 64 instances with 500 nodes per episode, 10,000 episodes, 20 considered solutions
 641 ($|\mathcal{K}| = 20$), and 10 rollouts per instance ($N_{roll} = 10$).

642 D.1 Sampling of the Exploration Weight during Training

643 Initially, we experimented with uniform sampling of the exploration weight. However, as shown in
 644 Figure 4a, this approach failed to adequately cover the Pareto front. To address this, we employed a
 645 Beta distribution with parameters $\alpha = \beta = 0.2$. This U-shaped distribution emphasizes the sampling
 646 of extreme exploration weights (close to 0 and 1), which proved crucial for the cNC to effectively
 647 learn the boundaries of the Pareto front (Figure 4b).

648 Furthermore, we conducted a comparative study against a configuration using multiple independently
 649 trained networks. In this baseline, we discretized the exploration preference into 11 values (0.0, 0.1,
 650 ..., 1.0) and trained a separate model for each. This required training 11 distinct networks. The results
 651 presented in Figure 4c demonstrate that the cNC is able to provide solutions that slightly dominate
 652 those obtained by independently trained networks.

Algorithm 2 cNC - Training Procedure

Input: Distribution of instances \mathcal{D} , number of training episodes E , number of rollouts N_{roll} , number of considered solutions $|\mathcal{K}|$, cNC policy π with parameters θ , batch size B

Training:

Initialize policy network π_θ

for episode $e = 1$ to E **do**

- $\mathcal{I} \leftarrow$ Sample a batch of B problem instances from \mathcal{D}
- $\mathcal{K} \leftarrow$ Initialize $|\mathcal{K}|$ random solutions
- $\omega \leftarrow$ Sample random exploration weight $\in [0, 1]$
- for** each instance i in the batch **do**

 - $x_i \leftarrow (\mathcal{I}, \mathcal{K}, \omega)$ {Define input state}
 - $l_i \leftarrow \pi_\theta(x_i)$ {Compute logits}
 - $p_i \leftarrow \text{Softmax}(l_i)$ {Compute probabilities}
 - for** $r = 1$ to N_{roll} **do**

 - $s_i^r \leftarrow \text{Rollout}(p_i)$ {Sample a solution}
 - $R_{\text{obj}}^i \leftarrow f(s_i^r)$
 - $R_{\text{dist}}^i \leftarrow \text{ComputeDistance}(s_i^r, \mathcal{K})$
 - $R_i^r \leftarrow (1 - \omega) \cdot R_{\text{obj}}^i + \omega \cdot R_{\text{dist}}^i$

 - end for**

- end for**

Policy Update:

$b_i \leftarrow \frac{1}{N_{roll}} \sum_{r=1}^{N_{roll}} R_i^r$ {per-instance baseline}

$A_i^r \leftarrow R_i^r - b_i$ {advantage}

$\theta \leftarrow \theta + \eta \sum_{i=1}^B \sum_{r=1}^{N_{roll}} \nabla_\theta(\log \pi_\theta(s_i^r | x_i)) A_i^r$

end for

Output: Trained policy parameters θ

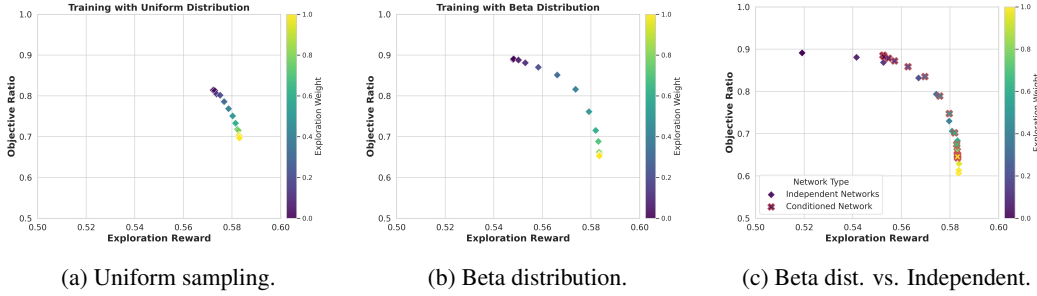
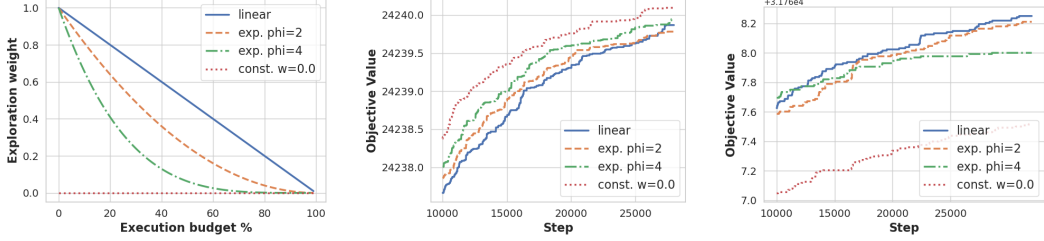


Figure 4: Bi-objective performance of different strategies. The plots show the objective value ratio with respect to the best known value (y-axis), against the exploration reward, computed as the average distance to the considered solutions (x-axis), for various exploration weights (colored points). Results are obtained on 100 ER graphs with 100 nodes for the MC problem. (a) cNC trained with uniform sampling of the exploration weight. (b) cNC trained with Beta distribution sampling ($\alpha = \beta = 0.2$). (c) Comparison between the Beta-trained cNC and multiple independently trained networks, each optimized for a specific, discretized exploration weight.

653 **D.2 Cooling Schedule**

654 Once trained the cNC, it permits to dynamically adjust the exploration weight throughout the optimization process. In the initial phases of the optimization process, a strong emphasis on exploration
 655 allows the algorithm to investigate a diverse set of solutions. As the process progresses, it becomes
 656 advantageous to gradually shift the focus towards exploitation. This transition can be seen as a
 657 cooling schedule, analogous to the temperature reduction in simulated annealing [Kirkpatrick et al.,
 658 1983].

660 Equation 4 presents the general formula for the cooling schedule, which dynamically adjusts the
 661 weight assigned to exploration based on the budget left. We investigated several cooling strategies,



(a) Different cooling schedules. (b) Avg. obj. curves for ER700-800 (c) Avg obj. curves for RB800-1200

Figure 5: Different cooling schedules for the exploration weight and their performance in ER700-800 and RB800-1200 evaluation datasets for the MC.

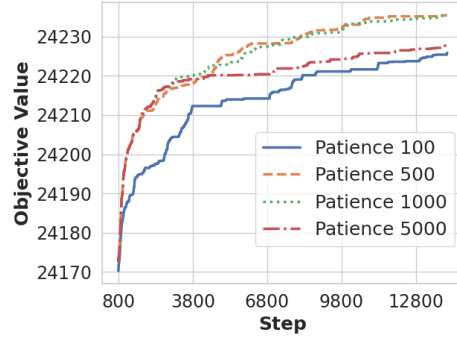


Figure 6: Influence of the Patience Parameter (N_{patience}) on Optimization Performance. The plot shows the evolution of the best objective value found during the optimization process for different values of N_{patience} (100, 500, 1000, and 5000) averaged over 128 ER700-800 graphs for the Maximum Cut problem.

662 modifying the cooling factor ϕ . We compare the linear cooling used in the paper ($\phi = 1$), with two
 663 exponential schedules ($\phi = 2$ and $\phi = 4$), where the exponential decrease of the weight should
 664 allow for a faster reduction in exploration compared to linear cooling, and a constant weight ($\omega = 0$)
 665 meaning that the policy only focuses on exploitation.

666 Figure 5a visualizes the cooling curves for each proposed schedule. We evaluated their performance
 667 on two distinct MC datasets: ER700-800 (Figure 5b) and RB800-1200 (Figure 5c).

668 Our results reveal a strong relationship between the optimal level of exploration and whether the
 669 evaluation data are drawn from the training distribution (ER) or from a different distribution (RB).
 670 For example, the strategy focused solely on exploitation ($\omega = 0$) performs best on the in-distribution
 671 ER graphs but exhibits the worst performance on the out-of-distribution RB graphs. This trend
 672 extends to the other cooling schedules. Higher exploration rates lead to improved performance on the
 673 out-of-distribution RB graphs, while lower exploration rates (emphasizing exploitation) yield better
 674 results on the in-distribution ER graphs. These findings underscore the importance of exploration for
 675 generalization to unseen data.

676 E Router Patience

677 The patience parameter (N_{patience}) is crucial for the router’s ability to balance exploitation and
 678 exploration in agent behavior. It specifies the number of consecutive iterations in which an agent can
 679 fail to improve its solution before being redirected to the Exploration Module to restart the search.
 680 Selecting an appropriate N_{patience} involves a trade-off: a low value can cause premature exploration,
 681 potentially missing out on good solutions, while a high value can result in excessive computation
 682 within a local region of the search space without yielding significant improvements.

Algorithm 3 MALOTE Inference Procedure

```
1: Input: Instance to be solved  $\mathcal{I}$ , trained NI and cNC policies, population size  $|\mathcal{A}|$ , max steps  $T_{\max}$ , patience threshold  $N_{\text{patience}}$ , initial exploration weight  $\omega_{\text{start}}$ , cooling factor  $\phi$ ,
2: Initialize:
3: for each agent  $i \in \mathcal{A}$  do
4:    $s_i^0 \leftarrow \text{RandomInitialization}(\mathcal{I})$ ,  $c_i \leftarrow 0$  {Consecutive non-improving steps}
5: end for
6:  $\mathcal{M}_0 \leftarrow \emptyset$  {Shared memory},  $s_{\text{best}} \leftarrow \emptyset$  {Stores the best solution found so far}
7: for  $t \leftarrow 1$  to  $T_{\max}$  do
8:   for each agent  $i \in \mathcal{A}$  do
9:     if  $c_i \geq N_{\text{patience}}$  then
10:       $\omega \leftarrow \omega_{\text{start}} \left(1 - \frac{t}{T_{\max}}\right)$  {Update exploration weight using cooling schedule}
11:       $\mathcal{K}_t \leftarrow \text{SelectSubset}(\mathcal{M}_t)$  {Select a subset of solutions from memory for exploration}
12:       $s_i^{t+1} \leftarrow \pi_{\text{cNC}}(\mathcal{I}, \mathcal{K}_t, \omega)$  {New solution via Exploration Module}
13:       $c_i \leftarrow 0$  {Reset counter}
14:    else
15:       $s_i^{t+1} \leftarrow \pi_{\text{NI}}(\mathcal{I}, s_i^t, \mathcal{M}_t)$  {Improve solution applying a bit-flip}
16:      if  $\text{IsImproved}(s_i^{t+1}, s_i^t)$  then
17:         $c_i \leftarrow 0$  {Reset counter}
18:      else
19:         $c_i \leftarrow c_i + 1$  {Increase counter}
20:      end if
21:    end if
22:     $\mathcal{M}_{t+1} \leftarrow \text{UpdateMemory}(\mathcal{M}_t, s_i^{t+1})$  {Update shared memory with new solution}
23:     $s_{\text{best}} \leftarrow \text{SelectBetter}(s_{\text{best}}, s_i^{t+1})$  {Update the best solution found}
24:  end for
25: end for
26: Output:  $s_{\text{best}}$ 
```

683 To determine suitable values for N_{patience} , we evaluated the performance of our method with several
684 different patience settings: 100, 500, 1000, and 5000; in the ER700-800 graph dataset. Our findings
685 indicate that a small patience value (e.g., $N_{\text{patience}} = 100$) hinders performance by prematurely
686 interrupting the search. Conversely, a large patience value (e.g., $N_{\text{patience}} = 5000$) results in slow
687 convergence, as agents persist in local search for too long. In this experiment, optimal performance
688 was achieved with patience values between 500 and 1000, which yielded similar results. Based on
689 these observations, setting the patience to the number of nodes in the graph instance serves as a
690 simple yet effective rule of thumb. The results of this ablation study are presented in Figure 6.

691 **F Pseudocode for MALOTE Inference**

692 Algorithm 3 presents the inference procedure of MALOTE, as described in Section 4. Lines 2-8 detail
693 the initialization of the agents, memory structures, and other key components. The main execution
694 loop, spanning lines 9-27, governs the core interaction and learning process.
695 Although the pseudo-code illustrates an inner loop that processes each agent sequentially, the actual
696 implementation executes these iterations in parallel.

697 **G Neural Network Architecture**

698 In this section, we detail the neural network architecture employed in our methodology.
699 Although the MALOTE framework is designed to be modular and compatible with various en-
700 coder architectures, including Graph Neural Networks (GNNs) and transformer-based models that
701 embed node and edge features into a latent space, we adopt the Graph Transformer (GT) archi-
702 tecture [Dwivedi and Bresson, 2020] due to its strong empirical performance across a range of
703 combinatorial optimization problems.
704 GTs extend the standard transformer model [Vaswani et al., 2017] to operate directly on graph-
705 structured data. Unlike traditional transformers, which are tailored for sequential inputs, GTs

706 incorporate structural information from the graph by integrating edge features, typically derived from
 707 the adjacency matrix, into their attention computations. In our implementation, GTs are combined
 708 with a Feed-Forward Neural Network (FFNN) decoder to parameterize both the NI and cNC policies.

709 G.1 Initial Projection

710 First, we extract the node and edge features as detailed in Appendix A for the problems addressed, and
 711 in Appendix B for additional problems. These features are then projected into a shared embedding
 712 space of dimension d to initialize the representations:

$$\mathbf{h}^{(0)} = \mathbf{W}_{\text{node}} \mathbf{x} + \mathbf{b}_{\text{node}}, \quad (11)$$

$$\mathbf{e}^{(0)} = \mathbf{W}_{\text{edge}} \mathbf{y} + \mathbf{b}_{\text{edge}}, \quad (12)$$

713 where $\mathbf{x} \in \mathbb{R}^{d_{\text{node}}}$ and $\mathbf{y} \in \mathbb{R}^{d_{\text{edge}}}$ are the node and edge feature vectors, respectively; $\mathbf{W}_{\text{node}} \in \mathbb{R}^{d \times d_{\text{node}}}$
 714 and $\mathbf{W}_{\text{edge}} \in \mathbb{R}^{d \times d_{\text{edge}}}$ are learnable weight matrices; $\mathbf{b}_{\text{node}} \in \mathbb{R}^d$ and $\mathbf{b}_{\text{edge}} \in \mathbb{R}^d$ are bias vectors;
 715 and $\mathbf{h}^{(0)} \in \mathbb{R}^d$ and $\mathbf{e}^{(0)} \in \mathbb{R}^d$ denote the initial node and edge embeddings.

716 G.2 Graph Transformer Layers

717 The GT consists of L layers that iteratively refine the node embeddings. Each GT layer comprises
 718 two main components: a multi-head self-attention mechanism and a FFNN, both followed by
 719 normalization layers.

720 **Multi-Head Self-Attention.** Within each GT layer, node embeddings are transformed into Query
 721 (Q), Key (K), and Value (V) tensors for each attention head. Assuming a multi-head attention
 722 mechanism with h heads and per-head dimension $d_k = \frac{d}{h}$, the transformations are defined as:

$$Q_i = \mathbf{W}_Q^{(i)} \mathbf{h}, \quad K_i = \mathbf{W}_K^{(i)} \mathbf{h}, \quad V_i = \mathbf{W}_V^{(i)} \mathbf{h}, \quad (13)$$

723 for each head $i = 1, \dots, h$, where $\mathbf{W}_Q^{(i)} \in \mathbb{R}^{d_k \times d}$, $\mathbf{W}_K^{(i)} \in \mathbb{R}^{d_k \times d}$, and $\mathbf{W}_V^{(i)} \in \mathbb{R}^{d_k \times d}$ are learnable
 724 projection matrices for each head.

725 The multi-head attention mechanism within a GT layer is computed as follows:

$$\text{Attn}_i(Q_i, K_i, V_i) = \left(\text{softmax} \left(\frac{Q_i K_i^\top}{\sqrt{d_k}} + \mathbf{E}_i \right) \cdot \mathbf{E}_i \right) V_i, \quad (14)$$

726 where $\mathbf{E}_i \in \mathbb{R}^{|V| \times |V|}$ integrates edge features into the attention scores for head i . Specifically, \mathbf{E}_i is
 727 computed by applying a learnable transformation to the edge embeddings:

$$\mathbf{E}_i = \mathbf{W}_e^{(i)} \mathbf{e}^{(0)}, \quad (15)$$

728 where $\mathbf{W}_e^{(i)} \in \mathbb{R}^{|V| \times |V|}$ is a learnable weight matrix that maps edge embeddings to a weight matrix
 729 and a bias matrix to be multiplied and added to the attention scores, respectively.

730 The outputs from all attention heads are concatenated and projected back to the original embedding
 731 dimension using a learnable output matrix:

$$\text{MultiHead}(Q, K, V) = \text{Concat}(\text{Attn}_1, \dots, \text{Attn}_h) \mathbf{W}_O, \quad (16)$$

732 where $\mathbf{W}_O \in \mathbb{R}^{h \cdot d_k \times d}$ is a learnable weight matrix.

733 **Residual Connection and Normalization.** The attention output is combined with the original node
 734 embeddings \mathbf{h} via a residual connection, followed by a normalization function:

$$\mathbf{h}' = \text{Norm}(\mathbf{h} + \text{MultiHead}(Q, K, V)).$$

735 **Feedforward Neural Network.** Subsequent to the attention mechanism, each GT layer applies a
 736 FFNN:

$$\mathbf{h}'' = \text{FFNN}(\mathbf{h}') = \text{Norm}(\text{Act}(\mathbf{W}_1 \mathbf{h}')) \mathbf{W}_2, \quad (17)$$

737 where $\mathbf{W}_1 \in \mathbb{R}^{d_{\text{ff}} \times d}$ and $\mathbf{W}_2 \in \mathbb{R}^{d \times d_{\text{ff}}}$ are learnable weight matrices, Act is the activation function,
 738 and Norm denotes a normalization function.

739 **Final Residual Connection and Normalization.** The output of the FFNN is then combined with
 740 the previous normalized embeddings \mathbf{h}' through another residual connection, followed by a final
 741 normalization step:

$$\mathbf{h}^{(l+1)} = \text{Norm}(\mathbf{h}' + \mathbf{h}''). \quad (18)$$

742 G.3 Decoder

743 The output from the final GT layer is subsequently processed by an additional FFNN to generate
 744 action logits:

$$z_i = \mathbf{W}_{\text{decoder}} \mathbf{h}_i^{(L)}, \quad (19)$$

745 where $\mathbf{W}_{\text{decoder}} \in \mathbb{R}^{1 \times d}$ is a learnable weight matrix, that maps each node's embedding to a single
 746 scalar value.

747 These logits z_i are then normalized using a softmax function over all nodes to produce a probability
 748 distribution:

$$p_i = \frac{\exp(z_i)}{\sum_{j \in V} \exp(z_j)}, \quad (20)$$

749 where p_i represents the probability of selecting node i for a given action.

750 The interpretation of p_i depends on the setting:

- 751 • In the **NI** setting, p_i denotes the probability of flipping the state of node i .
 752 • In the **cNC** setting, it corresponds to the probability of assigning node i to the first subset.

753 If the action space is defined over **edges** rather than nodes, as mentioned in Appendix B for alternative
 754 problems, edge embeddings can be constructed by concatenating the final-layer embeddings of the
 755 two connected nodes:

$$\mathbf{e}_{ij} = [\mathbf{h}_i^{(L)} \parallel \mathbf{h}_j^{(L)}], \quad (21)$$

756 and passed through an edge-wise FFNN to obtain edge-level logits, and probabilities in the same
 757 manner.

Table 3: Selected Model Hyperparameters

Model Hyperparameter	Value
Number of layers (L)	3
Hidden dimension (d)	64
Number of heads (h)	8
FFNN hidden dimension	256
Activation function	GeLU
Normalization	LayerNorm
Dropout	0%

758 G.4 Hyperparameter Selection

759 Table 3 lists the hyperparameters used in our model. These were determined through a comprehensive
 760 hyperparameter study, where different NI models were trained for 10,000 episodes on instances
 761 ranging from 20 to 40 nodes, and using a batch size of 1024. We explored various hyperparameter
 762 configurations and present the performance results on 100 instances with sizes of 20, 60, 100, and
 763 200 nodes in Table 4.

764 H Implementation Details of Baseline Methods

765 In this section, we provide a more detailed description of the methods used in the experiments.

Table 4: Performance under variations from the used hyperparameter setting. We report the average objective value obtained when testing the NI model after the last epoch of training on ER graph instances with 20, 60, 100 and 200 nodes for the MC problem.

Setting	ER20	ER60	ER100	ER200
Used Config.	25.6	192.7	503.6	1896.9
<i>Number of Layers</i>				
$L = 2$	25.6	192.4	502.1	1856.7
$L = 4$	25.6	192.6	503.2	1881.4
<i>Hidden Dimension</i>				
$d = 128$	25.6	192.6	502.7	1885.6
<i>Normalization</i>				
Instance	25.6	192.7	503.4	1894.6
RMS	25.6	192.6	503.2	1892.3
<i>Dropout</i>				
Dropout = 20%	25.6	192.7	503.2	1887.6

766 **Maximum Cut.** For the MC problem, we used the methods implemented in the Max Cut Benchmark [Nath and Kuhnle, 2024], modifying them to incorporate a time limit as a stopping criterion.
767 Specifically, we employed the GUROBI exact solver [Gurobi Optimization, LLC, 2023] which
768 is not able to obtain optimal solutions in the given budget, but provides an approximate solution.
769 We also used constructive heuristics such as Forward Greedy, which starts with an empty solution
770 and iteratively adds the vertex that provides the largest gain in the objective value. We applied
771 metaheuristic techniques including Tabu Search (TS) [Glover, 1990], which maintains a tabu list to
772 avoid revisiting recently explored solutions. The benchmark also includes learning-based methods,
773 including S2V-DQN [Khalil et al., 2017], a NC method guided by a GNN; ECO-DQN [Barrett
774 et al., 2020], a Neural Improvement variant of S2V-DQN; FlowNet [Zhang et al., 2023], a work that
775 samples from the solution space with Generative Flow Networks; and ANYCSP [Tönshoff et al.,
776 2023], a GNN-based search method for any constraint satisfaction problem.
777 Additionally, we integrated a Genetic Algorithm (GA) [Kramer and Kramer, 2017], a population-
778 based metaheuristic that evolves solutions through selection, crossover, and mutation operations;
779 Particle Swarm Optimization (PSO) [Kennedy and Eberhart, 1995], a swarm-based optimization
780 technique where a population of candidate solutions, called particles, moves through the solution
781 space guided by individual and collective experiences; BURER [Burer et al., 2002], a specialized
782 algorithm for MC that leverages semidefinite programming relaxations to approximate solutions;
783 and MARCO [Garmendia et al., 2024], a memory-based NCO method that uses a shared memory to
784 guide the search to unvisited solutions.

786 **Maximum Independent Set** We reused several methods also for MIS. We employed the GUROBI
787 exact solver, a greedy constructive heuristic that iteratively adds the node maximizing the gain while
788 ensuring feasibility to the MIS constraints. We also implemented a Genetic Algorithm, a PSO, and
789 used the MIS implementations of FlowNet and MARCO.
790 Apart from these benchmark methods, we included K_A MIS [Lamm et al., 2016], an evolutionary ap-
791 proach that combines graph kernelization, local search, and graph partitioning techniques to solve the
792 MIS problem. Furthermore, we integrated several learning-based methods: DGL [Böther et al., 2021]
793 and INTEL [Li et al., 2018], which combine a policy learnt by supervised learning with tree search;
794 LwD [Ahn et al., 2020], a scalable reinforcement learning framework that adaptively defers element-
795 wise decisions during solution generation to simplify hard decisions; and DiffUCO [Sanokowski et al.,
796 2024], a diffusion model using unsupervised learning to approximate intractable discrete distributions
797 without requiring training data.

798 **I Advantage of Centralized Training for Memory-Based Methods**

799 The NI model (from the improvement module) in our approach differs from MARCO [Garmendia
800 et al., 2024] in its training paradigm. While MARCO employs a decentralized training scheme in
801 which each search thread maintains a private memory, we utilize a centralized training framework
802 with a shared memory accessible to all agents.
803 We hypothesize that training with a shared memory increases the complexity of the learning task
804 for the NI model. The model must learn to navigate a more intricate decision-making landscape,
805 avoiding redundant actions not only within its own search trajectory, but also across the trajectories
806 of all other agents sharing the memory.

Table 5: Performance Comparison between decentralized (d) and centralized (c) training in MARCO.

Method	MC-objective ↑	MC-diversity ↑	MIS-objective ↑	MIS-diversity ↑
MARCO-d	24205.97	0.54	43.78	0.51
MARCO-c	24221.72	0.59	44.48	0.57

807 To isolate the impact of the centralized memory architecture on performance, we conducted a
808 controlled experiment. We trained a MARCO model using the original training hyperparameters
809 reported in [Garmendia et al., 2024], but modified the training process to incorporate a centralized,
810 shared memory, mirroring our approach. We then evaluated both the original decentralized MARCO
811 model (MARCO-d) and this centralized MARCO variant (MARCO-c) on the ER700-800 dataset for
812 both the MC and MIS problems.

813 Table 5 presents the results, comparing the average objective value and a measure of solution diversity.
814 Diversity is quantified using the average pairwise Hamming distance between the proposed solutions.
815 The results demonstrate that the centralized variant of MARCO, trained with the approach presented
816 in this paper, achieves significantly improved performance in terms of both the objective value and
817 the diversity of solutions, confirming that centralized memory is a key factor driving the performance
818 gains observed in our approach.

819 **J MALOTE as a Neural Population-Based Metaheuristic**

820 MALOTE shares several conceptual similarities with classical population-based metaheuristics such
821 as Genetic Algorithms (GA) and Particle Swarm Optimization (PSO). Like these methods, MALOTE
822 maintains a population of candidate solutions and iteratively improves them through interactions and
823 information sharing. In GA, this occurs via selection, crossover, and mutation; in PSO, particles
824 update their positions based on personal and global bests; in MALOTE, the population is updated
825 through neural policies conditioned on a centralized memory that captures the collective search
826 history. The key difference lies in how the update mechanisms are implemented: while GA and
827 PSO use hand-designed heuristics, MALOTE learns its update strategy end-to-end via reinforcement
828 learning, enabling adaptation to problem-specific structures. Additionally, MALOTE leverages neural
829 networks to encode graph-structured inputs and guide exploration, offering a more expressive and
830 learnable framework compared to the fixed dynamics of classical metaheuristics.

831 To highlight these differences in practice, we compare the anytime performance of MALOTE with
832 that of GA and PSO in Figure 7. This comparison evaluates how solution quality evolves over
833 time under equivalent computational budgets. The results demonstrate that MALOTE outperforms
834 classical metaheuristics having faster convergence, and converging in a higher quality solutions.

835 These findings support the view that data-driven learning can outperform traditional.

836 **J.1 Ablation Study**

837 To better understand the contribution of key components in the MALOTE architecture, we conduct an
838 ablation study focusing on the Exploration Module and the conditioned Neural Constructive (cNC)
839 policy. Specifically, we evaluate two simplified variants of MALOTE: (1) one without the Exploration
840 Module (denoted as MALOTE - {EM}), and (2) one where the Exploration Module is retained, but

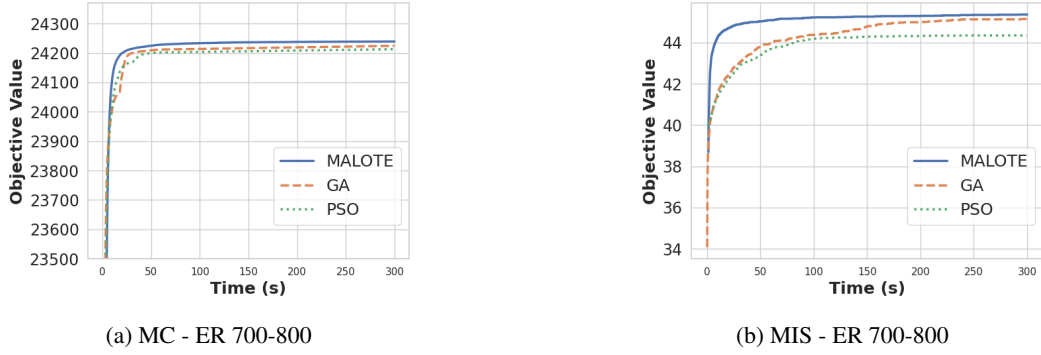


Figure 7: Anytime performance of MALOTE and population-based metaheuristics GA and PSO on MC and MIS problems. Each subplot shows the evolution of the best objective value found during the optimization process. Results are shown for both ER700-800 and RB800-1200 graph datasets.

841 the cNC policy is replaced with a random initialization strategy (denoted as MALOTE - {cNC}). We
 842 compare these configurations against the full MALOTE model, limiting each run to a fixed budget of
 843 $40|V|$ inference steps, where $|V|$ is the number of nodes in the instance.

Table 6 reports the final objective values obtained, their ratios relative to the best baselines shown in Table 1, and the average runtime required to complete $40|V|$ steps. The results confirm that both the Exploration Module and the cNC policy are critical for achieving strong optimization performance.

Furthermore, Figure 8 illustrates the anytime performance curves of MALOTE and its ablated variants. The results highlight the importance of the Exploration Module in continuously discovering high-quality solutions, and show that incorporating the cNC policy leads to better outcomes than relying on random sampling when the search begins to stagnate.

Table 6: Performance comparison on MC and MIS tasks for different ablation settings. The best overall results are highlighted in bold.

ER700-800				RB800-1200				
	Method	Type	Objective ↑	Ratio ↑	Time ↓	Objective ↑	Ratio ↑	Time ↓
MC	MALOTE - {EM}	RL / NI	24230.26	1.000	1.06m	31765.68	1.000	2.52m
	MALOTE - {cNC}	RL / NI	24237.23	1.000	3.46m	31767.60	1.000	6.10m
	MALOTE	RL / NI + cNC	24240.16	1.000	7.14m	31768.03	1.000	9.71m
MIS	MALOTE - {EM}	RL / NI	45.12	1.003	1.00m	40.40	0.936	2.10m
	MALOTE - {cNC}	RL / NI	45.29	1.006	5.31m	40.75	0.944	8.37m
	MALOTE	RL / NI + cNC	45.44	1.010	5.82m	41.04	0.951	8.94m

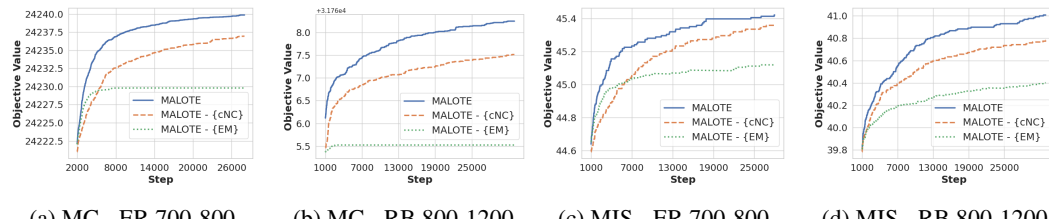


Figure 8: Anytime performance of MALOTE and ablations on MC and MIS problems. Each subplot shows the evolution of the best objective value found during the optimization process. Results are shown for both ER700-800 and RB800-1200 graph datasets.

851 NeurIPS Paper Checklist

852 1 Claims

853 Question: Do the main claims made in the abstract and introduction accurately reflect the
854 paper's contributions and scope?

855 Answer: [Yes]

856 Justification: The claims made are based on the experimental results.

857 Guidelines:

- 858 • The answer NA means that the abstract and introduction do not include the claims
859 made in the paper.
- 860 • The abstract and/or introduction should clearly state the claims made, including the
861 contributions made in the paper and important assumptions and limitations. A No or
862 NA answer to this question will not be perceived well by the reviewers.
- 863 • The claims made should match theoretical and experimental results, and reflect how
864 much the results can be expected to generalize to other settings.
- 865 • It is fine to include aspirational goals as motivation as long as it is clear that these goals
866 are not attained by the paper.

867 2. Limitations

868 Question: Does the paper discuss the limitations of the work performed by the authors?

869 Answer: [Yes]

870 Justification: Limitations and future work are discussed.

871 Guidelines:

- 872 • The answer NA means that the paper has no limitation while the answer No means that
873 the paper has limitations, but those are not discussed in the paper.
- 874 • The authors are encouraged to create a separate "Limitations" section in their paper.
- 875 • The paper should point out any strong assumptions and how robust the results are to
876 violations of these assumptions (e.g., independence assumptions, noiseless settings,
877 model well-specification, asymptotic approximations only holding locally). The authors
878 should reflect on how these assumptions might be violated in practice and what the
879 implications would be.
- 880 • The authors should reflect on the scope of the claims made, e.g., if the approach was
881 only tested on a few datasets or with a few runs. In general, empirical results often
882 depend on implicit assumptions, which should be articulated.
- 883 • The authors should reflect on the factors that influence the performance of the approach.
884 For example, a facial recognition algorithm may perform poorly when image resolution
885 is low or images are taken in low lighting. Or a speech-to-text system might not be
886 used reliably to provide closed captions for online lectures because it fails to handle
887 technical jargon.
- 888 • The authors should discuss the computational efficiency of the proposed algorithms
889 and how they scale with dataset size.
- 890 • If applicable, the authors should discuss possible limitations of their approach to
891 address problems of privacy and fairness.
- 892 • While the authors might fear that complete honesty about limitations might be used by
893 reviewers as grounds for rejection, a worse outcome might be that reviewers discover
894 limitations that aren't acknowledged in the paper. The authors should use their best
895 judgment and recognize that individual actions in favor of transparency play an impor-
896 tant role in developing norms that preserve the integrity of the community. Reviewers
897 will be specifically instructed to not penalize honesty concerning limitations.

898 3. Theory assumptions and proofs

899 Question: For each theoretical result, does the paper provide the full set of assumptions and
900 a complete (and correct) proof?

901 Answer: [NA]

902 Justification: The paper does not include theoretical results.

903 Guidelines:

- 904 • The answer NA means that the paper does not include theoretical results.

- 905 • All the theorems, formulas, and proofs in the paper should be numbered and cross-
 906 referenced.
 907 • All assumptions should be clearly stated or referenced in the statement of any theorems.
 908 • The proofs can either appear in the main paper or the supplemental material, but if
 909 they appear in the supplemental material, the authors are encouraged to provide a short
 910 proof sketch to provide intuition.
 911 • Inversely, any informal proof provided in the core of the paper should be complemented
 912 by formal proofs provided in appendix or supplemental material.
 913 • Theorems and Lemmas that the proof relies upon should be properly referenced.

914 **4. Experimental result reproducibility**

915 Question: Does the paper fully disclose all the information needed to reproduce the main ex-
 916 perimental results of the paper to the extent that it affects the main claims and/or conclusions
 917 of the paper (regardless of whether the code and data are provided or not)?

918 Answer: [Yes]

919 Justification: We are open sourcing the code to reproduce the experimental results.

920 Guidelines:

- 921 • The answer NA means that the paper does not include experiments.
- 922 • If the paper includes experiments, a No answer to this question will not be perceived
 923 well by the reviewers: Making the paper reproducible is important, regardless of
 924 whether the code and data are provided or not.
- 925 • If the contribution is a dataset and/or model, the authors should describe the steps taken
 926 to make their results reproducible or verifiable.
- 927 • Depending on the contribution, reproducibility can be accomplished in various ways.
 928 For example, if the contribution is a novel architecture, describing the architecture fully
 929 might suffice, or if the contribution is a specific model and empirical evaluation, it may
 930 be necessary to either make it possible for others to replicate the model with the same
 931 dataset, or provide access to the model. In general, releasing code and data is often
 932 one good way to accomplish this, but reproducibility can also be provided via detailed
 933 instructions for how to replicate the results, access to a hosted model (e.g., in the case
 934 of a large language model), releasing of a model checkpoint, or other means that are
 935 appropriate to the research performed.
- 936 • While NeurIPS does not require releasing code, the conference does require all submis-
 937 sions to provide some reasonable avenue for reproducibility, which may depend on the
 938 nature of the contribution. For example
 - 939 (a) If the contribution is primarily a new algorithm, the paper should make it clear how
 940 to reproduce that algorithm.
 - 941 (b) If the contribution is primarily a new model architecture, the paper should describe
 942 the architecture clearly and fully.
 - 943 (c) If the contribution is a new model (e.g., a large language model), then there should
 944 either be a way to access this model for reproducing the results or a way to reproduce
 945 the model (e.g., with an open-source dataset or instructions for how to construct
 946 the dataset).
 - 947 (d) We recognize that reproducibility may be tricky in some cases, in which case
 948 authors are welcome to describe the particular way they provide for reproducibility.
 949 In the case of closed-source models, it may be that access to the model is limited in
 950 some way (e.g., to registered users), but it should be possible for other researchers
 951 to have some path to reproducing or verifying the results.

952 **5. Open access to data and code**

953 Question: Does the paper provide open access to the data and code, with sufficient instruc-
 954 tions to faithfully reproduce the main experimental results, as described in supplemental
 955 material?

956 Answer: [Yes]

957 Justification: We are making public the source code of MALOTE.

958 Guidelines:

- 959 • The answer NA means that paper does not include experiments requiring code.
 960 • Please see the NeurIPS code and data submission guidelines (<https://nips.cc/public/guides/CodeSubmissionPolicy>) for more details.
 961 • While we encourage the release of code and data, we understand that this might not be
 962 possible, so “No” is an acceptable answer. Papers cannot be rejected simply for not
 963 including code, unless this is central to the contribution (e.g., for a new open-source
 964 benchmark).
 965 • The instructions should contain the exact command and environment needed to run to
 966 reproduce the results. See the NeurIPS code and data submission guidelines (<https://nips.cc/public/guides/CodeSubmissionPolicy>) for more details.
 967 • The authors should provide instructions on data access and preparation, including how
 968 to access the raw data, preprocessed data, intermediate data, and generated data, etc.
 969 • The authors should provide scripts to reproduce all experimental results for the new
 970 proposed method and baselines. If only a subset of experiments are reproducible, they
 971 should state which ones are omitted from the script and why.
 972 • At submission time, to preserve anonymity, the authors should release anonymized
 973 versions (if applicable).
 974 • Providing as much information as possible in supplemental material (appended to the
 975 paper) is recommended, but including URLs to data and code is permitted.

976 **6. Experimental setting/details**

977 Question: Does the paper specify all the training and test details (e.g., data splits, hyper-
 978 parameters, how they were chosen, type of optimizer, etc.) necessary to understand the
 979 results?

980 Answer: [Yes]

981 Justification: We carefully detail all the parameters in the appendix.

982 Guidelines:

- 983 • The answer NA means that the paper does not include experiments.
 984 • The experimental setting should be presented in the core of the paper to a level of detail
 985 that is necessary to appreciate the results and make sense of them.
 986 • The full details can be provided either with the code, in appendix, or as supplemental
 987 material.

988 **7. Experiment statistical significance**

989 Question: Does the paper report error bars suitably and correctly defined or other appropriate
 990 information about the statistical significance of the experiments?

991 Answer: [Yes]

992 Justification: We provide information regarding the intra-instance variability of non-
 993 deterministic methods, and inter-instance variability of all the methods.

994 Guidelines:

- 995 • The answer NA means that the paper does not include experiments.
 996 • The authors should answer “Yes” if the results are accompanied by error bars, confi-
 997 dence intervals, or statistical significance tests, at least for the experiments that support
 998 the main claims of the paper.
 999 • The factors of variability that the error bars are capturing should be clearly stated (for
 1000 example, train/test split, initialization, random drawing of some parameter, or overall
 1001 run with given experimental conditions).
 1002 • The method for calculating the error bars should be explained (closed form formula,
 1003 call to a library function, bootstrap, etc.).
 1004 • The assumptions made should be given (e.g., Normally distributed errors).
 1005 • It should be clear whether the error bar is the standard deviation or the standard error
 1006 of the mean.
 1007 • It is OK to report 1-sigma error bars, but one should state it. The authors should
 1008 preferably report a 2-sigma error bar than state that they have a 96% CI, if the hypothesis
 1009 of Normality of errors is not verified.

- 1012 • For asymmetric distributions, the authors should be careful not to show in tables or
1013 figures symmetric error bars that would yield results that are out of range (e.g. negative
1014 error rates).
1015 • If error bars are reported in tables or plots, The authors should explain in the text how
1016 they were calculated and reference the corresponding figures or tables in the text.

1017 **8. Experiments compute resources**

1018 Question: For each experiment, does the paper provide sufficient information on the com-
1019 puter resources (type of compute workers, memory, time of execution) needed to reproduce
1020 the experiments?

1021 Answer: [Yes]

1022 Justification: We provide the hardware and execution time necessary to execute the experi-
1023 ments.

1024 Guidelines:

- 1025 • The answer NA means that the paper does not include experiments.
1026 • The paper should indicate the type of compute workers CPU or GPU, internal cluster,
1027 or cloud provider, including relevant memory and storage.
1028 • The paper should provide the amount of compute required for each of the individual
1029 experimental runs as well as estimate the total compute.
1030 • The paper should disclose whether the full research project required more compute
1031 than the experiments reported in the paper (e.g., preliminary or failed experiments that
1032 didn't make it into the paper).

1033 **9. Code of ethics**

1034 Question: Does the research conducted in the paper conform, in every respect, with the
1035 NeurIPS Code of Ethics <https://neurips.cc/public/EthicsGuidelines>?

1036 Answer: [Yes]

1037 Justification: The NeurIPS Code of Ethics has been reviewed, and the paper conforms it in
1038 every aspect.

1039 Guidelines:

- 1040 • The answer NA means that the authors have not reviewed the NeurIPS Code of Ethics.
1041 • If the authors answer No, they should explain the special circumstances that require a
1042 deviation from the Code of Ethics.
1043 • The authors should make sure to preserve anonymity (e.g., if there is a special consid-
1044 eration due to laws or regulations in their jurisdiction).

1045 **10. Broader impacts**

1046 Question: Does the paper discuss both potential positive societal impacts and negative
1047 societal impacts of the work performed?

1048 Answer: [NA]

1049 Justification: There is no societal impact of the work performed.

1050 Guidelines:

- 1051 • The answer NA means that there is no societal impact of the work performed.
1052 • If the authors answer NA or No, they should explain why their work has no societal
1053 impact or why the paper does not address societal impact.
1054 • Examples of negative societal impacts include potential malicious or unintended uses
1055 (e.g., disinformation, generating fake profiles, surveillance), fairness considerations
1056 (e.g., deployment of technologies that could make decisions that unfairly impact specific
1057 groups), privacy considerations, and security considerations.
1058 • The conference expects that many papers will be foundational research and not tied
1059 to particular applications, let alone deployments. However, if there is a direct path to
1060 any negative applications, the authors should point it out. For example, it is legitimate
1061 to point out that an improvement in the quality of generative models could be used to
1062 generate deepfakes for disinformation. On the other hand, it is not needed to point out
1063 that a generic algorithm for optimizing neural networks could enable people to train
1064 models that generate Deepfakes faster.

- 1065 • The authors should consider possible harms that could arise when the technology is
1066 being used as intended and functioning correctly, harms that could arise when the
1067 technology is being used as intended but gives incorrect results, and harms following
1068 from (intentional or unintentional) misuse of the technology.
1069 • If there are negative societal impacts, the authors could also discuss possible mitigation
1070 strategies (e.g., gated release of models, providing defenses in addition to attacks,
1071 mechanisms for monitoring misuse, mechanisms to monitor how a system learns from
1072 feedback over time, improving the efficiency and accessibility of ML).

1073 **11. Safeguards**

1074 Question: Does the paper describe safeguards that have been put in place for responsible
1075 release of data or models that have a high risk for misuse (e.g., pretrained language models,
1076 image generators, or scraped datasets)?

1077 Answer: [NA]

1078 Justification: The paper poses no such risks.

1079 Guidelines:

- 1080 • The answer NA means that the paper poses no such risks.
1081 • Released models that have a high risk for misuse or dual-use should be released with
1082 necessary safeguards to allow for controlled use of the model, for example by requiring
1083 that users adhere to usage guidelines or restrictions to access the model or implementing
1084 safety filters.
1085 • Datasets that have been scraped from the Internet could pose safety risks. The authors
1086 should describe how they avoided releasing unsafe images.
1087 • We recognize that providing effective safeguards is challenging, and many papers do
1088 not require this, but we encourage authors to take this into account and make a best
1089 faith effort.

1090 **12. Licenses for existing assets**

1091 Question: Are the creators or original owners of assets (e.g., code, data, models), used in
1092 the paper, properly credited and are the license and terms of use explicitly mentioned and
1093 properly respected?

1094 Answer: [NA]

1095 Justification: The paper does not use existing assets from other authors.

1096 Guidelines:

- 1097 • The answer NA means that the paper does not use existing assets.
1098 • The authors should cite the original paper that produced the code package or dataset.
1099 • The authors should state which version of the asset is used and, if possible, include a
1100 URL.
1101 • The name of the license (e.g., CC-BY 4.0) should be included for each asset.
1102 • For scraped data from a particular source (e.g., website), the copyright and terms of
1103 service of that source should be provided.
1104 • If assets are released, the license, copyright information, and terms of use in the
1105 package should be provided. For popular datasets, paperswithcode.com/datasets
1106 has curated licenses for some datasets. Their licensing guide can help determine the
1107 license of a dataset.
1108 • For existing datasets that are re-packaged, both the original license and the license of
1109 the derived asset (if it has changed) should be provided.
1110 • If this information is not available online, the authors are encouraged to reach out to
1111 the asset's creators.

1112 **13. New assets**

1113 Question: Are new assets introduced in the paper well documented and is the documentation
1114 provided alongside the assets?

1115 Answer: [NA]

1116 Justification: The paper does not release new assets.

1117 Guidelines:

- 1118 • The answer NA means that the paper does not release new assets.
- 1119 • Researchers should communicate the details of the dataset/code/model as part of their
- 1120 submissions via structured templates. This includes details about training, license,
- 1121 limitations, etc.
- 1122 • The paper should discuss whether and how consent was obtained from people whose
- 1123 asset is used.
- 1124 • At submission time, remember to anonymize your assets (if applicable). You can either
- 1125 create an anonymized URL or include an anonymized zip file.

1126 **14. Crowdsourcing and research with human subjects**

1127 Question: For crowdsourcing experiments and research with human subjects, does the paper

1128 include the full text of instructions given to participants and screenshots, if applicable, as

1129 well as details about compensation (if any)?

1130 Answer: [NA]

1131 Justification: The paper does not involve crowdsourcing nor research with human subjects.

1132 Guidelines:

- 1133 • The answer NA means that the paper does not involve crowdsourcing nor research with
- 1134 human subjects.
- 1135 • Including this information in the supplemental material is fine, but if the main contribu-
- 1136 tion of the paper involves human subjects, then as much detail as possible should be
- 1137 included in the main paper.
- 1138 • According to the NeurIPS Code of Ethics, workers involved in data collection, curation,
- 1139 or other labor should be paid at least the minimum wage in the country of the data
- 1140 collector.

1141 **15. Institutional review board (IRB) approvals or equivalent for research with human**

1142 **subjects**

1143 Question: Does the paper describe potential risks incurred by study participants, whether

1144 such risks were disclosed to the subjects, and whether Institutional Review Board (IRB)

1145 approvals (or an equivalent approval/review based on the requirements of your country or

1146 institution) were obtained?

1147 Answer: [NA]

1148 Justification: The paper does not involve crowdsourcing nor research with human subjects.

1149 Guidelines:

- 1150 • The answer NA means that the paper does not involve crowdsourcing nor research with
- 1151 human subjects.
- 1152 • Depending on the country in which research is conducted, IRB approval (or equivalent)
- 1153 may be required for any human subjects research. If you obtained IRB approval, you
- 1154 should clearly state this in the paper.
- 1155 • We recognize that the procedures for this may vary significantly between institutions
- 1156 and locations, and we expect authors to adhere to the NeurIPS Code of Ethics and the
- 1157 guidelines for their institution.
- 1158 • For initial submissions, do not include any information that would break anonymity (if
- 1159 applicable), such as the institution conducting the review.

1160 **16. Declaration of LLM usage**

1161 Question: Does the paper describe the usage of LLMs if it is an important, original, or

1162 non-standard component of the core methods in this research? Note that if the LLM is used

1163 only for writing, editing, or formatting purposes and does not impact the core methodology,

1164 scientific rigorosity, or originality of the research, declaration is not required.

1165 Answer: [NA]

1166 Justification: The research does not involve LLMs

1167 Guidelines:

- 1168
- The answer NA means that the core method development in this research does not involve LLMs as any important, original, or non-standard components.
- 1169
- Please refer to our LLM policy (<https://neurips.cc/Conferences/2025/LLM>) for what should or should not be described.
- 1170
- 1171